MCB Accepted Manuscript Posted Online 2 January 2019
Mol. Cell. Biol. doi:10.1128/MCB.00376-18

Common and Differential Transcriptional Actions of Nuclear Receptors LXRα and LXRβ in macrophages

Ana Ramón-Vázquez[1,2,†], Juan Vladimir de la Rosa[1,2,†], Carlos Tabraue[2], Felix Lopez[2], Bonifacio Nicolas Díaz-Chico[2], Lisardo Bosca[1,2], Peter Tontonoz[3], Susana Alemany[1,2] and Antonio Castrillo[1,2,*]

[1]Instituto de Investigaciones Biomédicas "Alberto Sols," Consejo Superior de Investigaciones Científicas (CSIC)-Universidad Autónoma de Madrid, Madrid 28029, Spain.
[2]Unidad de Biomedicina (Unidad Asociada al CSIC), Instituto Universitario de Investigaciones Biomédicas y Sanitarias, Grupo de Investigación Medio Ambiente y Salud, Universidad de Las Palmas de Gran Canaria, Las Palmas 35016, Spain.
[3]Department of Pathology and Laboratory Medicine, University of California Los Angeles, California (UCLA), 90095; Los Angeles, CA USA.

[†] Ana Ramón-Vázquez and Juan Vladimir de la Rosa contributed equally to this work and should be considered as joint first authors.

*To whom correspondence should be addressed.
Antonio Castrillo, Ph.D.
Instituto de Investigaciones Biomédicas "Alberto Sols" CSIC-Universidad Autónoma de Madrid, Spain and Unidad de Biomedicina (Unidad Asociada al CSIC), Instituto Universitario de Investigaciones Biomédicas y Sanitarias (IUIBS) de la Universidad de Las Palmas de Gran Canaria (ULPGC).
Address: Arturo Duperier, 4. 28029 MADRID, Spain
Tel: +34 914975418
Fax: +34 915854401
Email: **acastrillo@iib.uam.es**

ABSTRACT

The liver X receptors, LXRα and LXRβ, are oxysterol-activated transcription factors that coordinately regulate gene expression important for cholesterol and fatty acid metabolism. In addition to their roles in lipid metabolism, LXRs participate in the transcriptional regulation of macrophage activation and are considered potent regulators of inflammation. LXR receptors are highly similar and, despite notable exceptions, most of their reported functions are substantially overlapping. However, their individual genomic distribution and transcriptional capacities have not been characterized. Here we report a macrophage cellular model expressing equivalent levels of tagged LXRs. ChIP-seq data analysis revealed that LXRα and LXRβ occupy both overlapping and exclusive genomic regulatory sites of target genes and also control the transcription of a receptor-exclusive set of genes. Analysis of genomic H3K27 acetylation and mRNA transcriptional changes in response to synthetic agonist or antagonist treatments revealed a putative mode of pharmacological-independent regulation of transcription. Integration of microarray and sequencing data enabled the description of three possible mechanisms of LXR transcriptional activation. Together, these results contribute to our understanding of the common and differential genomic actions of LXRs and their impact on biological processes in macrophages.

INTRODUCTION

Macrophages are professional phagocytic cells that play crucial roles in immune processes such as pathogen clearance and cytokine secretion, but they also perform other important functions in the regulation of metabolism and maintenance of tissue homeostasis (38). Macrophages exhibit a unique genetic plasticity, particularly at the precursor stage, when myeloid progenitors from different ontogenetic origins (yolk sac, fetal liver, adult blood monocytes) can give rise to most types of tissue macrophages (55). Transcriptional control of macrophage gene expression is orchestrated by a crosstalk between myeloid-specific master regulators, a small set of lineage-determining transcription factors, and chromatin remodelling enzymes involved in epigenetic modifications, all acting on key enhancer genomic regions (16, 18, 48). Recent studies have also demonstrated that adult macrophages from different anatomic locations present a particular transcriptional profile that is decisively determined by their local environment (32).

The liver X receptors, LXRα and LXRβ (encoded by *Nr1h3* and *Nr1h2* respectively), are transcription factors belonging to the nuclear receptor superfamily that bind to the DNA as obligate heterodimers with the retinoid X receptors (RXR). LXRs are sterol-sensing transcription factors that play essential roles in lipid and cholesterol metabolism and the immune response (47, 60, 62). LXRs control the expression of several genes that are pivotal for reverse cholesterol transport, fatty acid and phospholipid metabolism. Several studies have demonstrated that LXRα activity is predominant in the control of cholesterol and fatty acid metabolism in the liver (19, 39, 65) where its expression is markedly higher than LXRβ. LXRα is also expressed in adipose tissue, intestine, kidney and macrophages (62). On the other hand, LXRβ is expressed ubiquitously (45). Naturally occurring cholesterol derivatives, named oxysterols, have been shown to be potent LXR activators *in vitro* and *in vivo* (11, 24, 25, 34, 49). *In vivo* administration of synthetic LXR ligands has shown beneficial effects in several animal models of disease, including atherosclerosis, Alzheimer´s disease and psoriasis ((27) and reviewed in (20)). In addition, however, LXR ligands promote an elevation of plasma triglyceride levels and liver steatosis due to hepatic induction of the master regulator of the lipogenic pathway, SREBP1c (encoded by *Srebf1)* (44, 64). Ever since these discoveries, the design of LXRβ-specific synthetic agonists to treat metabolic disorders or inflammatory diseases, avoiding de novo lipogenesis, has been a challenging effort (47). Interestingly, recent studies have shown promising therapeutic potential of novel compounds (28, 29) with immunomodulatory and antineoplasic activities (51).

LXRα and LXRβ proteins share 77% of sequence homology and most gene regulatory functions are believed to be performed similarly by LXRα and LXRβ (45). Initial studies, using electrophoretic mobility shift assays (EMSA) and promoter analyses identified direct repeats of the classic nuclear receptor-binding motif AGGTCA separated by four nucleotides (DR4) as high-affinity binding sites for LXR-RXR heterodimers (62). This sequence binding preference has largely been confirmed by previous genome-wide chromatin immunoprecipitation experiments. However, these initial ChIP-seq analyses were performed in cells expressing unequal levels of LXRα and LXRβ and antibodies that do not discriminate between the two LXRs (9, 40, 49, 57).

Receptor-exclusive functions have been described for LXRα, such as transcriptional control of *Cd5l* expression (26), or the differentiation of the splenic marginal zone macrophages (2). Transcriptional regulation of target gene expression orchestrated preferentially by LXRβ has also been described (4, 35, 59). However, most LXR isoform-specific functions have been ascribed to the prominent expression of a particular receptor in a given cell type. A detailed analysis of specific LXRα and LXRβ transcriptional actions has not been conducted to date.

In this study, we developed a macrophage cellular model that stably expresses FLAG-tagged versions of either LXRα or LXRβ in an LXR-deficient background. Reconstituted cells were used to dissect LXR individual transcriptional actions and binding pattern dynamics to mouse genome, upon targeting with commonly used synthetic LXR agonist and antagonist. Using microarray data in combination with ChIP-sequencing data, we identify novel mechanisms of LXR-mediated gene activation, involving LXR pharmacological-dependent and -independent activation. This approach will contribute to better characterize LXRα and LXRβ common and differential genomic actions that further impact biological processes in macrophages.

MATERIALS AND METHODS

Mice

WT, LXRα-deficient (*Nr1h3*$^{-/-}$), LXRβ-deficient (*Nr1h2*$^{-/-}$) and LXRα/β-deficient (*Nr1h3*$^{-/-}$, *Nr1h2*$^{-/-}$) (denoted as LXR-DKO) mice on a mixed Sv129/C57BL/6 were originally provided by David Mangelsdorf (UTSW) (39). All mice were maintained under pathogen-free conditions in a temperature-controlled room and a 12-hour light-dark cycle in the animal facilities of Universidad de Las Palmas de Gran Canaria, ULPGC. All animal studies were conducted in accordance with institutional participants' animal ethics research committees (protocol CEEA-ULPGC 2015-002 and resolution 414-2015-ULPGC).

Cell culture and macrophage differentiation

Thioglycollate-elicited peritoneal macrophages were obtained through injection of 3mL of 3% sterile thioglycollate (BD Difco) pH 7.0 and after 3 days macrophages were collected after washing 3 times the peritoneal cavity with cold PBS. All cells were cultured in Dulbecco´s Modified Eagle´s medium (DMEM, Lonza) supplemented with 10% fetal bovine serum (Gibco), penicillin (100U/ml) (Sigma) and streptomycin (100µg/ml) (Sigma). For BMDM cell differentiation, bone marrow from femur and tibiae of 5 to 7 week-old WT or LXR-DKO mice was isolated and cultured for 7 days in DMEM supplemented with 10% conditioned medium containing M-CSF or GM-CSF and 1% antibiotics (penicillin and streptomycin) (Sigma).

Immortalization of murine macrophages from bone marrow and expression of FLAG-tagged LXRα and LXRβ receptors

Bone marrow-derived macrophages were immortalized using J2 retrovirus as previously described (7, 8, 23). Ectopic expression of LXRα or LXRβ was performed with pBabe-based retroviral expression system. Briefly, Phoenix A cells at 90% confluence were transfected with the pBabe-3FLAG-LXRα or pBabe-3FLAG-LXRβ vector (10), expressing either LXRα or LXRβ nuclear receptors and carrying antibiotic resistance to ampicillin and puromycin. For transfection, 10µg of plasmid and Lipofectamine 2000 (Thermo Fisher Scientific) 1:1.5 were used. After 6 hours, the culture medium is replaced with complete DMEM medium, which is collected after 48 hours containing the viral particles. Before exposing iBMDM-LXR-DKO cell culture to the viral supernatant, it was filtered through a 45µm pore size filter and mixed with 10µg/ml Polybrene® (SIGMA). Cells were cultured with Puromycin (SIGMA-Aldrich, 2-10 ug/ml gradually) for 2 weeks. Several clones expressing LXRα or LXRβ were isolated and tested for similar expression using anti-FLAG M2 antibody. A detailed protocol of this procedure is available through a recent review (42).

Treatment with LXR synthetic ligands

Pharmacological treatments were used as follows: 1µM synthetic LXR ligand GW3965 (12) and synthetic LXR antagonist GSK1440233A (denoted here as GW233) were both from Glaxo SmithKline (66) 1µM in DMSO (Sigma) stock solution. Additionally, cells were subjected to cholesterol biosynthesis inhibitor culture conditions: serum-free DMEM medium, supplemented with 0.2% bovine serum albumin (BSA, Sigma) and 2µM Zaragozic acid (squalene synthase inhibitor, Sigma) for 4 hours, prior to the exposure to the synthetic treatments.

Western blot

Whole-cell protein extracts were obtained with radioimmunoprecipitation assay buffer (RIPA, 10mM Tris-HCl pH7.5, 150mM NaCl, 1%Triton X-100, 0.5% sodium deoxycholate and 0.1% SDS and protease inhibitor (Complete®, Roche). Protein extracts were resolved by SDS-PAGE and transferred to PVDF membranes (Bio-Rad). Primary antibodies that recognize ABCA1 (Novus, NB400-105), ABCG1 (Novus, NB400-132), FLAG M2 (Sigma, F3165), LXRα/β (kindly provided by Knut R. Steffensen, Karolinska Institute,(40)), β-ACTIN (Santa Cruz, sc-47778, C4), GAPDH (Sigma, G9545) were used. Secondary antibodies were horseradish peroxidase-coupled (HRP) anti-mouse and anti-rabbit (Santa Cruz, sc-2005 and sc-2004). Reactive bands were detected by Clarity Western ECL substrate® (Bio-Rad). One representative western blot from three independent experiments is shown in each case.

Chromatin immunoprecipitation (ChIP) assay

ChIP assay for the study of LXR cistrome and variations in the acetylation status of the lysine 27 on histone H3 (H3K27ac) was performed as follows. Cell fixation and crosslinking was performed as in two steps: $2.5x10^7$ macrophages were fixed with 2μM disuccinimidyl glutarate (ThermoFisher Scientific) in PBS for 30 minutes. Next, cells were washed with PBS, and fixed for another 10 minutes with 1% methanol-free formaldehyde (ThermoFisher Scientific). Cross-linking reaction was quenched adding glycine to a final concentration of 200mM (Sigma). Chromatin extraction was performed in a two-step lysis reaction: a hypotonic buffer was used for nuclei extraction (50mM Tris-HCl pH8, 85mM KCl, 0.5% NP-40, supplemented with Complete® (Roche) protease inhibitor). Secondly, chromatin was resuspended in lysis buffer (50mM Tris-HCl pH8, 10mM EDTA, 1% SDS, Complete®) and stored at -80ºC. Finally, chromatin was sonicated with Diagenode Bioruptor® sonication device for 60 minutes (30 sec ON/30 sec OFF) to generate 200-400bp fragments and 10% of the total volume was set aside to test fragment size (input material). Immunoprecipitation was performed with 4μg of anti-FLAG M2 antibody or anti-H3K27ac (Abcam, ab4729) on 2ml of previously diluted chromatin with dilution buffer (10mM Tris-HCl pH8, 2mM EDTA, 1% Triton™ X-100, 150mM NaCl and 5% glycerol). Protein-bound immune complexes were captured with 100μg of magnetic Dynabeads® Protein A (Thermo-Fisher Scientific). Unbound complexes were washed out with 3 buffers of increasing ionic strength: 20mM Tris-HCl pH8, 2mM EDTA pH8, 1% Triton™ X-100, 0.1% SDS and 150mM (first buffer) or 500mM NaCl (second buffer) 10mM Tris-HCl, 1% sodium deoxycholate, 1mM EDTA pH8, 1% NP-40, 250mM LiCl (third buffer), followed by 2 washes with TE buffer (10mM Tris-HCl pH8, 1mM EDTA pH8). DNA fragments were reverse-crosslinked 30 minutes at 37ºC in 1% SDS, 0.1M $NaHCO_3$, 10μL of 5M NaCl, 6μg/ml RNase A and 1 hour at 55ºC with 400μg/ml proteinase K (Takara). Column purification was performed with Qiagen® QIAquick PCR Purification Kit and DNA was eluted in a final volume of 50μL, 5μL of which were used for qPCR amplification. Primers used for ChIP-qPCR analysis are listed in Supplementary Table 7.

High-throughput sequencing

ChIP DNA was quantified using Qubit 2.0 fluorometer. To prepare libraries, a minimum of 2ng of DNA anti-FLAG-immunoprecipitated and 1-2ng of anti-H3K27Ac-immunoprecipitated DNA was pooled from 5 biological replicates per condition. Libraries were prepared by the Genomics Unit of the Centre de Regulacion Genomica (CRG, Barcelona, Spain) using the NEBNext Ultra DNA Library Prep kit for Illumina (Ref#7370) following the manufacture instructions. 12 cycles of PCR were done for the final library amplification for all samples. Sequencing was performed using Illumina HiSeq2000 equipment. For ChIP-Seq, sequencing data (single-end 50 bp reads), obtained from Ilumina HiSeq 2000, were aligned to UCSC mm10 genome using bowtie2 aligner (v2.2.9)(31). Each ChIP-Seq experiment was normalized to a total number of 107 uniquely mapped tags. Aligned read files were visualized with IGV (52)genome browser and analyzed with HOMER software, http://homer.ucsd.edu/homer/ (v4.9). LXR peaks in each experiment were identified using HOMER comparing to data obtained from LXR-DKO samples as negative control (18). Peak list was further filtered using a tag-count cut-off of 40. This number was chosen by comparing the average tag count found in LXR peaks in each experiment. LXRs peaks and H3K27Ac regions were clustered and represented as tag densities heatmap within a window of 4 Kb around the LXR peaks using SEQminer (63). Ontology analysis of each LXR peak cluster was performed with DAVID Bioinformatics resource (21). Details of all applied bioinformatic analytical tools are available in a recent review protocol on this particular data processing (14). Gene Set Enrichment Analysis (GSEA) was used to correlate genes expression data with LXR ChIP-seq data. GSEA (50) analysis was performed using two lists: a pre-ranked gene expression list obtained from microarray analysis and a list of genes obtained from the annotation of ChIP-seq peaks to the neighbouring genes found on a window of +/- 50 Kb using BedTools (41) and the mouse genome annotation of UCSC mm10.

RNA extraction, cDNA synthesis and real-time qPCR

Total RNA was extracted from iBMDM-LXR-DKO or iBMDM-LXRα/-LXRβ, using TRI Reagent® (MRC) following product specifications. RNA pellet was resuspended with DEPC-treated water and 1µg was used for retrotranscription with iScript cDNA Synthesis kit™ (Bio-Rad). For RT qPCR assay, 5µL of cDNA was mixed with 15µL of 2X PCR MasterMix (Diagenode), and 0.4µM qPCR primer mix. Primers used for qPCR analysis are listed in Supplementary Table 7. Fluorescence emission was captured with the thermal cycler CFX connect™ (Bio-Rad). The relative levels of RNA were calculated according to the ΔΔCt method and individual expression data was normalized to 36B4 expression.

Microarray analysis and Biological pathway analysis

Changes in RNA expression promoted by ligand treatment (GW3965 and GW233) in immortalized macrophages were analyzed using GeneChip® Mouse Gene 2.0 ST Array (Affymetrix). Raw expression values, obtained as Log_2 and normalized to reference genes, were processed by the Genomic Unit of the Complutense University of Madrid. Heatmap representations were performed according to logarithmic-transformed values (Log_2) of fold change expression and arranged in decreasing order of magnitude. Gene Ontology Biological Process Analysis (GO BP terms) and Ingenuity Pathway Analysis (IPA®) were performed on transcripts classified in the three heatmap categories, under program default settings. Only significant terms (p-value>10^{-2}) are shown.

Molecular and Cellular Biology

207 **Statistical analysis**

208 Real-time quantitative PCR expression measurements and immunoprecipitated fragment amplification
209 were presented as mean (SD), calculated from three biological replicates. Statistical differences with
210 reference conditions were analyzed with unpaired t-test (*p<0.05 and **p<0.01)

RESULTS

LXRα and LXRβ expression and activity in macrophage culture *in vitro* models.

Traditionally, LXR-specific biological functions in the macrophage have been characterized using pharmacological strategies combined with genetic receptor deficiency. However, the relative expression levels of the LXRα and LXRβ proteins in most prior studies was not carefully defined, and in many cases LXRα and LXRβ protein levels were simply assumed to be equivalent across different macrophage populations. We examined the protein expression of LXRα and LXRβ in thioglycollate-elicited peritoneal and bone marrow-derived macrophages, differentiated with M-CSF (macrophage colony-stimulating factor) or GM-CSF (granulocyte-macrophage colony-stimulating factor) (Figure 1A). The highest expression of LXRα was found in elicited peritoneal macrophages, followed by M-CSF-derived macrophages, whereas the lowest LXRα expression was displayed by GM-CSF-derived cells. In contrast, LXRβ was similarly expressed across all the tested macrophage types. These results were further confirmed by real-time qPCR (Figure 1B). Additionally, we found that endogenous LXRs displayed post-transcriptional protein stabilization when exposed to the synthetic LXR agonist GW3965, in agreement with previous reports describing these effects in human cells (22). We also found that the degree of target gene induction varied with the type of macrophage (Figure 1B).

Next, we used an LXR-specific agonist and antagonist (GW3965 and GW233, respectively) to study LXR actions in WT, LXR double knockout (*Nr1h3*$^{-/-}$/*Nr1h2*$^{-/-}$) and single knockout (*Nr1h3*$^{-/-}$ or *Nr1h2*$^{-/-}$) primary peritoneal macrophages. As expected, GW3965 was able to effectively induce the expression of *Abca1* and *Abcg1*, in LXR-WT peritoneal macrophages, but its activity was completely abolished in the presence of GW233 (Figure 1C). In contrast, these drugs were ineffective in LXR-DKO cells which, conversely, displayed elevated levels of ABCA1 and ABCG1 proteins in agreement with previous reports (46, 58). Secondly, the ability of GW233 to effectively target each of the LXR nuclear receptors was tested in cells expressing only LXRα or LXRβ (Figure 1D). GW233 blocked the expression of *Abca1* and *Abcg1* to the same extent in LXRα$^{-/-}$ and LXRβ$^{-/-}$ cells. These results establish the pharmacological action of GW233 in primary murine macrophages, showing its ability to effectively target both LXRα and LXRβ nuclear receptors.

Ectopic expression of LXRα and LXRβ in immortalized macrophages (iBMDM).

To be able to pinpoint common and LXR receptor-specific transcriptional actions and to gain better insight into the molecular interaction networks underlying LXR biological effects, we developed an immortalized bone marrow-derived macrophage cell model expressing one LXR receptor at a time. Initially, an immortalized LXR-DKO bone marrow macrophage cell line was established as described (7, 23, 43). Next, the expression of LXRα and LXRβ receptors was reconstituted separately in this LXR-DKO parental cell line, in order to obtain two additional immortalized cell lines (Figure 2A). The virally-expressed LXR proteins were tagged with FLAG (3xFLAG-LXR) to normalize LXR protein recognition in both cell lines using FLAG antibody. We selected FLAG-positive clones exhibiting similar expression of LXRα and LXRβ. Importantly, we also selected for lines in which the level of LXR protein expression was not excessively higher than in primary peritoneal macrophages (Figure 2B and 2C). Because in vitro primary BMDM and many in vivo tissue macrophages present low levels of LXRα expression (32),

we used elicited peritoneal macrophages to compare with our clones. For simplicity, these immortalized cell lines will be referred to as iBMDM-LXR-DKO, iBMDM-LXRα and iBMDM-LXRβ. Reconstituted LXR cells effectively induced target genes such as *Abca1*, *Abcg1* and others upon agonist treatment with GW3965 (Figure 2B and C). As expected, the induction of LXRα-specific target gene *Cd5l* (also known as AIM (37)), analyzed by real-time qPCR, was only observed in iBMDM-LXRα line upon stimulation with GW3965 (Figure 2C). Thus, we developed and validated model cell lines with defined levels of LXR receptor expression that respond to pharmacological stimulation, inducing target genes in the presence of agonist and repressing in the presence of an antagonist.

LXRα- and LXRβ-specific binding and H3K27 acetylation through targeted chromatin immunoprecipitation (ChIP).

We optimized ChIP conditions for these macrophage lines using the monoclonal FLAG M2 antibody and targeted qPCR amplification of known LXR target gene regulatory sequences (Figure 3A). To verify the effect of agonistic and antagonistic functions of GW3965 and GW233 on LXR binding ability, iBMDM cell lines were stimulated with GW3965 or GW233 (both 1 μM) for 24 hours. LXR binding in the regulatory regions of selected target genes was assessed by ChIP-qPCR (Figure 3B). We did not find differences in LXR binding to their DNA target sequences when comparing agonist vs antagonist treatments. However, since these synthetic molecules promote protein stabilization, it is possible that liganded LXRs exhibit increased LXR-DNA interactions when comparing to vehicle, non-treated control cells.

We analyzed histone H3 tail acetylation (H3K27ac) at the regulatory genomic regions of known LXR target genes, under agonist or antagonist stimulation. The alternating presence and absence of this histone mark under these treatments is indicative of cycles of highly accessible chromatin and compaction, associated with transcriptional activation and repression. Immunoprecipitation of acetylated regions was verified by qPCR in iBMDM LXR-expressing lines (Figure 3C). Acetylation levels of regulatory regions of LXR targets were strongly dependent on the presence of agonist or antagonist (Figure 3C).

LXRα and LXRβ display distinctive genome-wide binding signatures.

In order to study the individual contribution of LXRα and LXRβ receptors to the LXR genomic landscape, we performed chromatin immunoprecipitation coupled to deep sequencing (ChIP-seq) in iBMDM-LXR-DKO, iBMDM-LXRα and iBMDM-LXRβ lines in response to GW3965. Details about peak calling, performed to discriminate background signal and false positives from significant LXR binding events, are given in materials and methods section. Surprisingly, sequencing analysis revealed extensive differences in the number of genomic binding sites of LXR receptors (Figure 4A and B). LXRβ was present at a total of 1,021 highly-confident genomic locations, whereas LXRα could be detected at 606. Of all the sites, 502 were common binding locations to both LXRs, which represent 49% of LXRβ sites and 83% of LXRα sites. These data indicate that a large proportion of LXRα in cultured macrophages is bound to genomic sites that can be occupied by LXRβ as well (“dual” sites). In sharp contrast, almost 50% LXRβ binding was observed at selective sites that were not occupied by LXRα. The genomic distribution of genomic peaks (in reference to TSS/TTS/exons/introns/intergenic regions)

was similar between receptors (Figure 4C). A complete list with all genomic locations of LXR peaks and their annotation to proximal genes is enumerated in supplementary table 1.

Next, we correlated the binding of LXR receptors in iBMDM-LXRα and iBMDM-LXRβ immortalized cell lines with that of their heterodimeric partner, retinoid X receptor alpha (RXRα). We compared RXRα ChIP-seq data obtained from public NCBI's GEO database (accession number GSE63698) with our LXRα/β ChIP-seq data (Figure 4D). As expected, RXRα receptor mapped to largely overlapping sites with LXR. RXRα peaks displayed higher tag counts in those genomic locations where LXRα and LXRβ were bound simultaneously (Figure 4E). Accordingly, LXR/RXRα binding locations could be classified into three clusters, depending on dual or alternatively, LXRα or LXRβ-selective peaks.

To further characterize the sequence composition of regions with LXR binding and to predict coexisting transcription factor binding, we performed *de novo* and known motif sequence analysis with HOMER software on the three LXR/RXRα-bound clusters (Figure 4F). Interestingly, LXR-binding clusters were associated with common and distinct pattern of transcription factor binding sequences (all motifs listed in Supplementary table 2). The most enriched known motif in all clusters was the DR-4 element (LXR response element, LXRE), followed by diverse nuclear receptor motifs in the LXRα/β and LXRβ clusters. *De novo* motif discovery analysis also revealed that LXRE and COUP-TFII motifs were the most robustly enriched sequence elements in all clusters. Strikingly, some sequence motifs, identified by either motif analysis strategy, were only significantly enriched in those peak set sequences bound exclusively by one LXR receptor. This was the case for PBX1, found in the LXRα-specific peak set and BATF or C/EBP, identified in the LXRβ cluster (Figure 4F and Supplementary table 2). The apparent interdependence between certain factors and specific LXR-bound peak sets suggests a collaborative binding mechanism in either direction. Given the differential motifs associated with the sequences contained in the LXR peak clusters, we performed Gene Ontology (GO) term enrichment analysis of the genes annotated to these sets of peaks (Supplementary table 3). Besides the expected functions related to cholesterol and lipid metabolism, other functions associated to leukocyte and non-immune cell homeostasis were found for the dual peak cluster. The LXR receptor-specific clusters were enriched for heterogeneous functions, most importantly, cell differentiation for the LXRα-specific cluster and DNA binding activity and signal transduction for the LXRβ cluster.

In order to gain a more comprehensive vision of the LXR genomic binding pattern and its relationship to transcriptional control of target gene expression, we performed H3K27ac ChIP-seq upon pharmacological treatment with GW3965 and GW233. As previously indicated, this epigenetic mark is a reliable indicator of active transcription (13, 17, 32). We used the same pharmacological strategy of agonist vs antagonist shown in Figure 3C (without a baseline, vehicle-treated control), in order to get the most relevant information between maximal activation and repression. Analysis of H3K27ac changes located within LXR-bound regions (representing a 2-kb window around the LXR peak centre), after 24-hour pharmacological treatment is presented as a density heatmap in Figure 5A. Surprisingly, we could identify two types of H3K27 acetylated regions: those pharmacologically responsive to synthetic compounds and those either poorly or non-responsive to pharmacological stimulation. Strikingly, the majority of the acetylated regions fell within this last category, in the three LXR-bound peak clusters. Accordingly, LXR peak-associated acetylated genomic regions could be further subdivided into clusters and arranged owing to pharmacological responsiveness (C1-2 for dual LXR-

bound peaks, C3-4 LXRα-selective and C5-6 LXRβ-selective) (Figure 5A). *De novo* motif analysis was performed with HOMER software on clusters C1 to C6 and the most representative predicted factors, with their associated p-values, are indicated for each cluster. Importantly, an LXRE site was the most enriched sequence motif found in all C1-C6 clusters. This finding clearly indicates that a bone fide classic LXR binding site (DR-4), and not indirect, alternative or degenerate sites, mediates the recruitment of LXRα and LXRβ to their functional genomic locations.

We next focused on acetylated regions that showed a clear correlation with LXR receptor binding, i.e. those where LXR receptor/s could be found at the core of the open chromatin region. Box plot representation of mean acetylation tag counts (Log_2) revealed that H3K27ac changes experienced similar variations with pharmacological treatments at locations where LXRα or LXRβ is present (clusters C1, C3, C5; Figure 5B, upper panel). These results indicate that analysis of H3K27ac changes, in the vicinity of LXR peak locations, does not distinguish relevant differences between LXRα and LXRβ transactivation power.

LXRα and LXRβ transcriptional profiling.

To explore the possibility that differential receptor binding was linked to the selective gene transcription profiles of LXRα and LXRβ in response to ligand, we performed genome-wide gene expression analysis with Mouse Gene 2.0 ST Affymetrix microarray, using RNA from cells stimulated with GW3965 (maximal activation) and GW233 (control, maximal repression). Expression data was relativized in two ways: 1) expression values in response to GW3965 were represented relative to GW233 treatment in each iBMDM macrophage cell line, and alternatively, 2) gene expression under each treatment condition was referenced to expression values obtained in iBMDM-LXR-DKO macrophages. One representation aimed to discover induced/repressed genes by synthetic compounds, and the second analysis focused on the analysis of genes induced/repressed by the ectopic expression of each LXR isoform relative to LXR-DKO control. Fold changes in transcript levels were depicted in separate heatmaps, depending on LXRα/β-, LXRα- or LXRβ-mediated (Figure 6, left, middle and right panels respectively) transcriptional control. The number of transcripts induced in each case is also indicated on the left side of each heatmap.

Our analysis revealed three possible transcriptional activation mechanisms or modes of action, that we designated I, II, III (heatmaps in Figure 6). Mode of action I involves transcript induction in a pharmacologically-responsive fashion, and derepressed expression of the transcript in the absence of LXR receptor/s. Expression of genes in this class is higher in iBMDM-LXR-DKO cells than that in LXR-expressing iBMDMs under antagonistic conditions (GW233). Mode II represents the canonical model for transcriptional activation, where agonist binding to the LXR/RXR heterodimer triggers a conformational change, displacing the corepressor complex and facilitating the interaction with coactivator complexes. Expression of transcripts is highly dependent on LXR pharmacological activation and concomitant presence of the LXR receptor/s in the macrophage cell. Consequently, expression of these genes is higher with GW3965 treatment than iBMDM-LXR-DKO cells. Lastly, induction of transcripts in mode III occurred in a pharmacologically non-responsive manner, but expression values were higher in LXR-expressing lines compared to iBMDM-LXR-DKO macrophages under both agonistic and antagonistic treatment conditions, therefore displaying a stark LXR receptor/s

dependence. Genome browser snapshots of representative genes and their associated acetylation modifications are shown below to illustrate each mode of action (Figure 6, lower panels).

We found ~100 transcripts upregulated jointly by LXRα and LXRβ after pharmacological activation (including mode I and mode II, Figure 6, top left). In contrast, GW3965-activated LXRα promoted the expression of a striking elevated number of genes (~1,500 transcripts; Figure 6, top part of middle heatmap). LXRβ activation induced the expression of ~450 genes (Figure 6, top part of right heatmap). Modes of action I and II comprised less upregulated transcripts than mode III in all receptor categories. Surprisingly, the number of transcripts regulated by LXRα was an order of magnitude higher than by LXRβ. These results highlight that LXRα, despite being present at reduced number of genomic locations than LXRβ, is able to promote transactivation of a wide collection of genes (Figure 6 middle). Collectively, these results provide the first indication that LXR nuclear receptors regulate gene expression through three distinct transcriptional modes of action.

Next, we assessed the global correlation between gene expression and LXRα and LXRβ occupancy. This type of analysis distinguishes putative targets that could be induced directly by the influence of a near LXR binding, or indirectly either by inducing the expression of other proteins or perhaps by a direct but distant regulation. We associated each LXR peak to the near upstream and downstream genes that appear within a 50 Kb window. This correlation delivered two lists of genes: genes proximal to LXRα binding locations and genes proximal to LXRβ binding locations (within +/- 50Kb window). The resulting gene lists were compared to our microarray gene expression profiling performed in iBMDM-3F-LXRα and iBMDM-3F-LXRβ respectively using ranked Gene Set Enrichment Analysis (GSEA). In both cases, GSEA analysis revealed that genes which present an LXR binding to their close proximity strongly clustered with genes that were up-regulated by GW3965 agonist in the microarray gene expression list (supplementary table 4, represented by red lines under the curve). Gene lists of each analysis (complete lists in supplementary table 4) show a high core enrichment score associated to those genes intensely regulated in the microarray. LXRα binding positively correlated with 138 genes regulated in the microarray, whereas LXRβ appears to be influencing the positive expression of 266 genes. These results suggest that LXRα modulates the expression of many genes possibly through indirect mechanisms (only 138/1,500 correlation), whereas LXRβ binding is present in the vicinity of many of its regulated genes (266/450). Globally, these correlation studies strongly support the idea that direct binding of LXR to genomic regions promotes the induction of gene expression and not gene repression.

Bioinformatic analysis of pharmacologically sensitive and insensitive LXR dual or isotype-selective targets.

We further assessed the contribution of LXR-regulated (either dual, or receptor-specific) genes to biological pathways in macrophages, focusing on the two main categories of mechanistically-related LXR transcriptional activation: pharmacologically responsive (modes I and II) and weakly/non-responsive (mode III). We performed Ingenuity® Pathway Analysis (IPA) and Gene Ontology (GO) Biological Process Enrichment bioinformatic analysis. Among the enriched functions for the pharmacologically-responsive category, we found that LXRα/β and LXRα, in addition to be implicated in lipid metabolism, were also linked with pathways such as the unfolded protein response and leukocyte migration, respectively. LXRβ was strongly associated with the acute-phase response and vesicle-

mediated transport (Figure 7A and Supplementary table 5). Analysis on the second category (mode III) yielded a totally different array of functions for each LXR receptor. This analysis linked the genes regulated by both LXRα and LXRβ (dually) to DNA replication and rRNA processing, LXRα-dependent genes to inflammatory responses, and LXRβ regulated genes to lymphocyte differentiation, among other functions (Figure 7B and Supplementary table 5).

We next sought to identify upstream signaling pathways and factors that had been implicated in the regulation of these biological processes, acting as signaling hubs and regulating transcription of these clusters of genes. This type of bioinformatic analysis would predict possible ways in which LXR activity is connected to signaling factors that control the expression of these clusters of genes. These regulator pathways may amplify LXR activation, or trigger parallel actions that activate biological pathways linked to LXR receptors. Within the pharmacologically-responsive category, we found diverse molecules, such as the LPS co-receptor CD14, the transcription factor EGR1, and the chemotactic protein S100A8 associated with the LXRα-specific signaling cascade. On the other hand, molecules connecting gene expression regulated by LXRβ-specific activation were principally cytokines or cytokine-related genes as IL-6, IL-1β, TNF or IL-10RA (Figure 8A and B). Thus, this data predicts that LXRα (ligand-dependent responses) may possibly be involved in TLR-dependent immune responses and LXRβ would likely participate in IL1, TNF signaling.

Interestingly, when we examined the computer prediction of molecular regulators of pharmacologically non-responsive signaling cascades, we found that LXRα-dependent mode III genes relied on few molecular regulators, particularly on IFNγ and TLR9, which displayed an extensive influence over a manifold of additional molecules, magnifying the initial activating event and triggering several signaling pathways (Figure 9A and B). On the other hand, LXRβ-dependent genes (insensitive to ligand stimulation) are connected through a wide variety of upstream molecules that display a more limited range of action, exemplified by TP53, ESRRγ, TCF3 and IL-2 (Figure 9B, right). A similar situation was found for both receptors LXRα/β, which appear to influence signaling pathways through ACKR2 and TREX1. Biological pathway activation by these molecules was also examined by IPA (Supplementary table 6).

DISCUSSION

LXRα and LXRβ are nuclear receptors that play a crucial role in the control of whole body cholesterol metabolism (33). Previous work from our laboratory and others has demonstrated that LXRs also participate in diverse aspects of macrophage transcriptional machinery, including inflammation and host defense (1, 47). Both LXRα and LXRβ proteins are present in macrophages, but their individual functions in macrophage models have not been conclusively addressed. Despite the fact that LXR activity has been extensively studied using synthetic agonists in culture systems, an absence of specific tools to isolate and manipulate LXRα and LXRβ proteins individually has limited our understanding of their specific roles in macrophage biological processes (6). Thus, the main objective of the present work was to characterize the distinctive transcriptional properties of LXRα and LXRβ in murine macrophages. Two main concepts arise from our study. The first is the striking difference in LXRα versus LXRβ genomic-binding landscapes, despite the similarity of their direct DNA-binding motifs. The second is the different biological consequences of specific LXR DNA-binding events that reflect distinct modes of transcriptional regulation.

Since naturally-occurring macrophage models express varying levels of LXRα versus LXRβ (Figure 1A-B of this work and reference (32)), we generated an immortalized macrophage cellular model (iBMDM) (7, 43) that expresses equivalent levels of each LXR receptor separately. This iBMDM model has proven to be an effective way to interrogate macrophage functions *in vitro*, as these cells display expression markers and consistent characteristics of functional macrophages (7). Our iBMDM system expressing FLAG-tagged LXRs, reconstituted on an LXR-DKO genetic background, allowed us to unambiguously define characteristic receptor functions. Moreover, we clarified the specific actions of potent, commercially available, pharmacological tools in this LXR reconstituted system: the non-steroidal LXR agonist GW3965, widely accepted as potent stimulator of LXR activity (12), and the synthetic LXR antagonist GW233 (66). We also tested the ability of GW233 to inhibit GW3965-dependent induction of target genes in LXR single-knockout macrophages, which confirmed its potent antagonistic effect on both LXRα and LXRβ. Our iBMDM system appropriately reproduces LXR responses shared by LXRα and LXRβ, such as induction of classical dual target genes (56), as well as individual LXRα-specific transcription of *Cd5l* (26, 54).

Our genome-wide ChIP-seq analysis of LXRα versus LXRβ binding revealed a common group of DNA regions that can be occupied by both LXRα and LXRβ, and a large set of distinctive LXRβ specific peaks. The frequency of LXRα-exclusive binding regions was surprisingly lower. Thus, despite the high degree of similarity between both receptors, LXRβ is able to bind to a higher number of sites than LXRα in the macrophage genome. We initially expected to find many sites selectively bound by LXRα, as exclusive actions linked to this receptor have been previously described *in vitro* and *in vivo* (2, 26, 54). Remarkably, our peak filtering strategy used LXR-null cells and input DNA as negative controls that resulted in a robust set of curated peaks that exhibit DR-4 LXR binding motifs as the most enriched sequence found in all binding sites. Because previous studies used cell lines with uneven levels of LXRs or antibodies that do not discriminate between LXRα and LXRβ, we believe that our datasets represent the most accurate LXR binding repertoire described for macrophages (9, 18, 40). Recently, it was reported that LXR genes arose through a gene duplication event (15). However, it is unclear

whether LXRα has acquired specialized functions related to lipid metabolism and immunity, losing its ability to regulate other genes, or whether an expansion of LXRβ-associated functions has occurred, resulting in LXRα occupying a reduced number of genomic sites in comparison.

It is noteworthy that our motif analysis identified accompanying sequences that were selectively associated with the binding of one LXR receptor in particular. For example, C/EBP-like sites were not found in the LXRα-specific peak set, whereas PBX1 sequences were absent in the LXRβ peak cluster. Interestingly, a signaling cascade dependent on an LXRα-C/EBPβ interaction has recently been described as important for insulin induction of SREBP1c in the liver (53). In addition, a cooperative mechanism of action has been previously described for complexes containing the homeodomain protein PBX1. Interaction of Hox transcription factors with PBX1 complexes was demonstrated to be necessary to modulate their binding specificity in *Drosophila* (36). More recently, PBX1 pioneer binding ability for non-permissive chromatin was identified in myoblasts, and this activity is believed to facilitate the targeting of MyoD for muscle lineage gene activation (5). It is possible that similar or distinctive interactions are also operating in macrophages. However, to prove the function of these factors in LXR-specific binding capacities, genetic manipulation of neighboring sequences and/or elimination of these factors will be necessary. Nevertheless, it is therefore plausible that, despite a canonical LXRE sequence being present in all of these LXR-specific clusters, the mutually-exclusive binding of each LXR receptor could be facilitated by interactions with a cohort of accessory factors that provide a permissive binding environment at these genomic locations.

We also used changes in H3K27 acetylation marks in response to agonist/antagonist as readout of transcriptional activation/repression differences between LXRs. Strikingly, we found that a remarkable number of the enhancer regions flanking LXR peaks displayed weak or no H3K27ac changes in response to pharmacological agonist/antagonist exposure. We hypothesize that this behavior is explained by one or a combination of the following possibilities: i) the presence of LXR on these locations is important to confer a certain level of H3K27ac mark but does not promote acetylation modifications in response to ligand; ii) LXR binding could be playing a mere bystander role in these pharmacological insensitive enhancer regions, and other factors could be critically contributing to the appearance of this acetylation marks, including pioneer factors or LDTFs (18).

Analysis of the microarray dataset broadened and complemented our ChIP-seq data interpretation. We defined three different groups of genes that were associated with distinct putative mechanisms of transcriptional regulation (referred to as I, II and III). These three activation modes were found to be employed by both LXRα and LXRβ. Mode I is the “derepression” mode, which is exemplified by the gold-standard LXR target, *Abca1*. Mode I gene expression is higher in LXR-DKO control conditions relative to the iBMDM-LXR lines, but their expression increases upon GW3965 stimulation (20). Mode II represents the canonical transcriptional activation mechanism that has been previously characterized in depth (46, 58), in which pharmacological responsiveness is accompanied by higher expression in LXRα or LXRβ-expressing macrophages relative to LXR-DKO line. Interestingly, a large set of genes found by expression comparison do not fall in these two “classic” modes, and we propose here a distinct mode of action, called mode III, which represents pharmacologically non-responsive transcriptional activation. Within this category of mode III, we observe that expression values of most genes do not respond to pharmacological antagonism with GW233 when compared to GW3965, but their expression is still

519 significantly higher than that observed in LXR-DKO cells. It is possible that ectopic overexpression of
520 LXRα or LXRβ, even if liganded by a potent antagonist, promotes the recruitment of coactivator
521 complexes that results in higher RNA expression levels of a large set of targets when compared to
522 similar conditions in LXR-DKO cells. However, future experiments are needed to directly test the
523 differential requirement of coregulators in modes I-II vs mode III LXR-regulated gene expression. As
524 mentioned above, this mode III comprises groups of transcripts regulated dually by both LXRα and
525 LXRβ, or exclusively by LXRα or LXRβ.
526 Our bioinformatics analyses suggested that LXRα and LXRβ may participate in specific biological
527 functions beyond fatty acid and steroid metabolism. For example, LXRα-selective gene regulation was
528 found to be linked to "apoptosis" and "leukocyte migration". Interestingly, we have recently
529 demonstrated that LXRs regulate leukocyte chemotaxis (3). It will be interesting to validate whether
530 LXRα has a prominent role over LXRβ in leukocyte migration. On the other hand, specific functions for
531 LXRβ identified by Gene Ontology and IPA analysis were linked to "selection of thymocytes" and
532 "lymphocyte differentiation". Remarkably, binding sites for BATF, which is important for lymphoid
533 progenitor and Th differentiation (30, 61), were enriched in the LXRβ-selective cluster. Thus, it is
534 possible that LXRβ cooperates with BATF in pathways related to lymphocyte activation. Processes
535 controlled by LXRβ in lymphocytes that regulate proliferation and the acquire immune response have
536 previously been reported (4).
537 In conclusion, our data provide compelling evidence that LXRα and LXRβ bind to both common and
538 distinct regulatory sequences in the genome and exert transcriptional control over a wide range of
539 macrophage pathways. Importantly, these studies highlight the importance of LXR receptors in direct
540 transcriptional regulation of immune-related functions. Moreover, the integration of our DNA binding and
541 RNA expression data reveal three distinct modes of transcriptional regulation by LXRs (depicted as
542 models in Figure 10). Particularly important is the recognition that most LXR target genes are not
543 responsive to ligand (mode III). In the future it will be important to link the specific LXRα and LXRβ
544 regulatory actions uncovered here to biological functions in different tissue-resident macrophage
545 populations, especially in the context of steady-state homeostasis or disease.

AVAILABILITY and ACCESSION NUMBERS

Datasets are available under accession series GSE104027.

ACKNOWLEDGEMENTS

We thank David Mangelsdorf (University of Texas, Southwestern, USA) for the LXR null mice, Knut R. Steffensen (Karolinska Institutet, Sweden) for the LXRα/β antibody. We are grateful to Luis del Peso (IIBM-UAM) for his suggestions on bioinformatic analysis. We also thank Jon Collins (GlaxoSmithKline SA North Carolina) for the LXR agonist and antagonist.

FUNDING

This work was supported by grants to A.C. laboratory from the Spanish Ministry of Economy and Competitiveness (MINECO) SAF2011-29244 and SAF2014-56819-R]; Grant for Networks of Excellence from MINECO "Nuclear Receptors in Cancer, Metabolism and Inflammation" (NuRCaMeIn) [SAF2015-71878-REDT and SAF2017-90604-REDT]. A.R-V. received a fellowship from MINECO reference number BES-2012-058574.

CONFLICT OF INTEREST

The authors declare that they have no conflict of interest.

REFERENCES

1. **A-Gonzalez, N., and A. Castrillo.** 2011. Liver X receptors as regulators of macrophage inflammatory and metabolic pathways. Biochim Biophys Acta **1812:**982-994.
2. **A-Gonzalez, N., J. A. Guillen, G. Gallardo, M. Diaz, J. V. de la Rosa, I. H. Hernandez, M. Casanova-Acebes, F. Lopez, C. Tabraue, S. Beceiro, C. Hong, P. C. Lara, M. Andujar, S. Arai, T. Miyazaki, S. Li, A. L. Corbi, P. Tontonoz, A. Hidalgo, and A. Castrillo.** 2013. The nuclear receptor LXRalpha controls the functional specialization of splenic macrophages. Nat Immunol **14:**831-9.
3. **Beceiro, S., A. Pap, Z. Czimmerer, T. Sallam, J. A. Guillen, G. Gallardo, C. Hong, A. G. N, C. Tabraue, M. Diaz, F. Lopez, J. Matalonga, A. F. Valledor, P. Dominguez, C. Ardavin, C. Delgado-Martin, S. Partida-Sanchez, J. L. Rodriguez-Fernandez, L. Nagy, P. Tontonoz, and A. Castrillo.** 2018. LXR nuclear receptors are transcriptional regulators of dendritic cell chemotaxis. Mol Cell Biol.
4. **Bensinger, S. J., M. N. Bradley, S. B. Joseph, N. Zelcer, E. M. Janssen, M. A. Hausner, R. Shih, J. S. Parks, P. A. Edwards, B. D. Jamieson, and P. Tontonoz.** 2008. LXR signaling couples sterol metabolism to proliferation in the acquired immune response. Cell **134:**97-111.
5. **Berkes, C. A., D. A. Bergstrom, B. H. Penn, K. J. Seaver, P. S. Knoepfler, and S. J. Tapscott.** 2004. Pbx marks genes for activation by MyoD indicating a role for a homeodomain protein in establishing myogenic potential. Mol Cell **14:**465-77.
6. **Bischoff, E. D., C. L. Daige, M. Petrowski, H. Dedman, J. Pattison, J. Juliano, A. C. Li, and I. G. Schulman.** 2010. Non-redundant roles for LXRalpha and LXRbeta in atherosclerosis susceptibility in low density lipoprotein receptor knockout mice. J Lipid Res **51:**900-6.
7. **Blasi, E., B. J. Mathieson, L. Varesio, J. L. Cleveland, P. A. Borchert, and U. R. Rapp.** 1985. Selective immortalization of murine macrophages from fresh bone marrow by a raf/myc recombinant murine retrovirus. Nature **318:**667-70.
8. **Blasi, E., D. Radzioch, S. K. Durum, and L. Varesio.** 1987. A murine macrophage cell line, immortalized by v-raf and v-myc oncogenes, exhibits normal macrophage functions. European Journal of Immunology **17:**1491-1498.
9. **Boergesen, M., T. A. Pedersen, B. Gross, S. J. van Heeringen, D. Hagenbeek, C. Bindesboll, S. Caron, F. Lalloyer, K. R. Steffensen, H. I. Nebb, J. A. Gustafsson, H. G. Stunnenberg, B. Staels, and S. Mandrup.** 2012. Genome-wide profiling of liver X receptor, retinoid X receptor, and peroxisome proliferator-activated receptor alpha in mouse liver reveals extensive sharing of binding sites. Mol Cell Biol **32:**852-67.
10. **Chen, M., S. Beaven, and P. Tontonoz.** 2005. Identification and characterization of two alternatively spliced transcript variants of human liver X receptor alpha. J Lipid Res **46:**2570-9.
11. **Chen, W., G. Chen, D. L. Head, D. J. Mangelsdorf, and D. W. Russell.** 2007. Enzymatic reduction of oxysterols impairs LXR signaling in cultured cells and the livers of mice. Cell Metab **5:**73-9.
12. **Collins, J. L., A. M. Fivush, M. A. Watson, C. M. Galardi, M. Lewis, L. Moore, D. Parks, J. Wilson, T. K. Tippin, J. G. Binz, K. D. Plunket, D. G. Morgan, E. J. Beaudet, K. D. Whitney, S. A. Kliewer, and T. M. Willson.** 2002. Identification of a nonsteroidal liver X receptor agonist through parallel array synthesis of tertiary amines. J Med Chem. **45:**1963-6.
13. **Creyghton, M. P., A. W. Cheng, G. G. Welstead, T. Kooistra, B. W. Carey, E. J. Steine, J. Hanna, M. A. Lodato, G. M. Frampton, P. A. Sharp, L. A. Boyer, R. A. Young, and R. Jaenisch.** 2010. Histone H3K27ac separates active from poised enhancers and predicts developmental state. Proc Natl Acad Sci U S A **107:**21931-6.
14. **de la Rosa, J., A. Ramón-Vázquez, C. Tabraue, and A. Castrillo.** 2018. Analysis of LXR Nuclear Receptor Cistrome through ChIP-seq Data Bioinformatics. Methods Mol Biol. **In press**.

15. **Fonseca, E., R. Ruivo, M. Lopes-Marques, H. Zhang, M. M. Santos, B. Venkatesh, and L. F. C. Castro.** 2017. LXRα and LXRβ nuclear receptors evolved in the common ancestor of gnathostomes. Genome biology and evolution**:**305.
16. **Glass, C. K., and G. Natoli.** 2016. Molecular control of activation and priming in macrophages. Nat Immunol **17:**26-33.
17. **Heintzman, N. D., G. C. Hon, R. D. Hawkins, P. Kheradpour, A. Stark, L. F. Harp, Z. Ye, L. K. Lee, R. K. Stuart, C. W. Ching, K. A. Ching, J. E. Antosiewicz-Bourget, H. Liu, X. Zhang, R. D. Green, V. V. Lobanenkov, R. Stewart, J. A. Thomson, G. E. Crawford, M. Kellis, and B. Ren.** 2009. Histone modifications at human enhancers reflect global cell-type-specific gene expression. Nature **459:**108-12.
18. **Heinz, S., C. Benner, N. Spann, E. Bertolino, Y. C. Lin, P. Laslo, J. X. Cheng, C. Murre, H. Singh, and C. K. Glass.** 2010. Simple combinations of lineage-determining transcription factors prime cis-regulatory elements required for macrophage and B cell identities. Mol Cell **38:**576-89.
19. **Hong, C., M. N. Bradley, X. Rong, X. Wang, A. Wagner, V. Grijalva, L. W. Castellani, J. Salazar, S. Realegeno, R. Boyadjian, A. M. Fogelman, B. J. Van Lenten, S. T. Reddy, A. J. Lusis, R. K. Tangirala, and P. Tontonoz.** 2012. LXRalpha is uniquely required for maximal reverse cholesterol transport and atheroprotection in ApoE-deficient mice. J Lipid Res **53:**1126-33.
20. **Hong, C., and P. Tontonoz.** 2014. Liver X receptors in lipid metabolism: opportunities for drug discovery. Nature Reviews Drug Discovery **13:**433-444.
21. **Huang, D. W., B. T. Sherman, Q. Tan, J. R. Collins, W. G. Alvord, J. Roayaei, R. Stephens, M. W. Baseler, H. C. Lane, and R. A. Lempicki.** 2007. The DAVID Gene Functional Classification Tool: a novel biological module-centric algorithm to functionally analyze large gene lists. Genome biology **8:**R183.
22. **Ignatova, I. D., J. Angdisen, E. Moran, and I. G. Schulman.** 2013. Differential regulation of gene expression by LXRs in response to macrophage cholesterol loading. Mol Endocrinol **27:**1036-47.
23. **Ito, A., C. Hong, X. Rong, X. Zhu, E. J. Tarling, P. N. Hedde, E. Gratton, J. Parks, and P. Tontonoz.** 2015. LXRs link metabolism to inflammation through Abca1-dependent regulation of membrane composition and TLR signaling. Elife **4:**e08009.
24. **Janowski, B. A., M. J. Grogan, S. A. Jones, G. B. Wisely, S. A. Kliewer, E. J. Corey, and D. J. Mangelsdorf.** 1999. Structural requirements of ligands for the oxysterol liver X receptors LXRalpha and LXRbeta. Proc Natl Acad Sci U S A **96:**266-71.
25. **Janowski, B. A., P. J. Willy, T. R. Devi, J. R. Falck, and D. J. Mangelsdorf.** 1996. An oxysterol signalling pathway mediated by the nuclear receptor LXR alpha. Nature **383:**728-31.
26. **Joseph, S. B., M. N. Bradley, A. Castrillo, K. W. Bruhn, P. A. Mak, L. Pei, J. Hogenesch, M. O'Connell R, G. Cheng, E. Saez, J. F. Miller, and P. Tontonoz.** 2004. LXR-dependent gene expression is important for macrophage survival and the innate immune response. Cell **119:**299-309.
27. **Joseph, S. B., A. Castrillo, B. A. Laffitte, D. J. Mangelsdorf, and P. Tontonoz.** 2003. Reciprocal regulation of inflammation and lipid metabolism by liver X receptors. Nat Med **9:**213-9.
28. **Kick, E., R. Martin, Y. Xie, B. Flatt, E. Schweiger, T. L. Wang, B. Busch, M. Nyman, X. H. Gu, G. Yan, B. Wagner, M. Nanao, L. Nguyen, T. Stout, A. Plonowski, I. Schulman, J. Ostrowski, T. Kirchgessner, R. Wexler, and R. Mohan.** 2015. Liver X receptor (LXR) partial agonists: biaryl pyrazoles and imidazoles displaying a preference for LXRbeta. Bioorg Med Chem Lett **25:**372-7.
29. **Kick, E. K., B. B. Busch, R. Martin, W. C. Stevens, V. Bollu, Y. Xie, B. C. Boren, M. C. Nyman, M. H. Nanao, L. Nguyen, A. Plonowski, I. G. Schulman, G. Yan, H. Zhang, X. Hou, M. N. Valente, R. Narayanan, K. Behnia, A. D. Rodrigues, B. Brock, J. Smalley, G. H. Cantor, J. Lupisella, P. Sleph, D. Grimm, J. Ostrowski, R. R. Wexler, T. Kirchgessner, and R. Mohan.** 2016. Discovery of Highly Potent Liver X Receptor beta Agonists. ACS Med Chem Lett **7:**1207-1212.

30. **Kurachi, M., R. A. Barnitz, N. Yosef, P. M. Odorizzi, M. A. Dilorio, M. E. Lemieux, K. Yates, J. Godec, M. G. Klatt, A. Regev, E. J. Wherry, and W. N. Haining.** 2014. The transcription factor BATF operates as an essential differentiation checkpoint in early effector CD8+ T cells. Nat Immunol **15:**373-83.
31. **Langmead, B., and S. L. Salzberg.** 2012. Fast gapped-read alignment with Bowtie 2. Nat Methods **9:**357-9.
32. **Lavin, Y., D. Winter, R. Blecher-Gonen, E. David, H. Keren-Shaul, M. Merad, S. Jung, and I. Amit.** 2014. Tissue-resident macrophage enhancer landscapes are shaped by the local microenvironment. Cell **159:**1312-26.
33. **Lee, S. D., and P. Tontonoz.** 2015. Liver X receptors at the intersection of lipid metabolism and atherogenesis. Atherosclerosis **242:**29-36.
34. **Lehmann, J. M., S. A. Kliewer, L. B. Moore, T. A. Smith-Oliver, B. B. Oliver, J. L. Su, S. S. Sundseth, D. A. Winegar, D. E. Blanchard, T. A. Spencer, and T. M. Willson.** 1997. Activation of the nuclear receptor LXR by oxysterols defines a new hormone response pathway. J Biol Chem **272:**3137-40.
35. **Mak, P. A., B. A. Laffitte, C. Desrumaux, S. B. Joseph, L. K. Curtiss, D. J. Mangelsdorf, P. Tontonoz, and P. A. Edwards.** 2002. Regulated expression of the apolipoprotein E/C-I/C-IV/C-II gene cluster in murine and human macrophages. A critical role for nuclear liver X receptors alpha and beta. The Journal of biological chemistry **277:**31900-8.
36. **Mann, R. S., and M. Affolter.** 1998. Hox proteins meet more partners. Curr Opin Genet Dev **8:**423-9.
37. **Miyazaki, T., Y. Hirokami, N. Matsuhashi, H. Takatsuka, and M. Naito.** 1999. Increased susceptibility of thymocytes to apoptosis in mice lacking AIM, a novel murine macrophage-derived soluble factor belonging to the scavenger receptor cysteine-rich domain superfamily. J Exp Med **189:**413-22.
38. **Okabe, Y., and R. Medzhitov.** 2016. Tissue biology perspective on macrophages. Nat Immunol **17:**9-17.
39. **Peet, D. J., S. D. Turley, W. Ma, B. A. Janowski, J. M. Lobaccaro, R. E. Hammer, and D. J. Mangelsdorf.** 1998. Cholesterol and bile acid metabolism are impaired in mice lacking the nuclear oxysterol receptor LXR alpha. Cell **93:**693-704.
40. **Pehkonen, P., L. Welter-Stahl, J. Diwo, J. Ryynänen, A. Wienecke-Baldacchino, S. Heikkinen, E. Treuter, K. R. Steffensen, and C. Carlberg.** 2012. Genome-wide landscape of liver X receptor chromatin binding and gene regulation in human macrophages. BMC genomics **13:**50.
41. **Quinlan, A. R., and I. M. Hall.** 2010. BEDTools: a flexible suite of utilities for comparing genomic features. Bioinformatics **26:**841-2.
42. **Ramón-Vázquez, A., J. de la Rosa, C. Tabraue, and A. Castrillo.** 2018. Bone Marrow-Derived Macrophage Immortalization of LXR Nuclear Receptor-Deficient Cells. Methods Mol Biol. **in press**.
43. **Rapp, U. R., J. L. Cleveland, T. N. Fredrickson, K. L. Holmes, H. C. Morse, 3rd, H. W. Jansen, T. Patschinsky, and K. Bister.** 1985. Rapid induction of hemopoietic neoplasms in newborn mice by a raf(mil)/myc recombinant murine retrovirus. J Virol **55:**23-33.
44. **Repa, J. J., G. Liang, J. Ou, Y. Bashmakov, J. M. Lobaccaro, I. Shimomura, B. Shan, M. S. Brown, J. L. Goldstein, and D. J. Mangelsdorf.** 2000. Regulation of mouse sterol regulatory element-binding protein-1c gene (SREBP-1c) by oxysterol receptors, LXRalpha and LXRbeta. Genes Dev **14:**2819-30.
45. **Repa, J. J., and D. J. Mangelsdorf.** 2000. The role of orphan nuclear receptors in the regulation of cholesterol homeostasis. Annu Rev Cell Dev Biol **16:**459-81.
46. **Repa, J. J., S. D. Turley, J. A. Lobaccaro, J. Medina, L. Li, K. Lustig, B. Shan, R. A. Heyman, J. M. Dietschy, and D. J. Mangelsdorf.** 2000. Regulation of absorption and ABC1-mediated efflux of cholesterol by RXR heterodimers. Science **289:**1524-9.
47. **Schulman, I. G.** 2017. Liver X receptors link lipid metabolism and inflammation. FEBS Lett **591:**2978-2991.

48. **Smale, S. T., A. Tarakhovsky, and G. Natoli.** 2014. Chromatin contributions to the regulation of innate immunity. Annu Rev Immunol **32:**489-511.

49. **Spann, N. J., L. X. Garmire, J. G. McDonald, D. S. Myers, S. B. Milne, N. Shibata, D. Reichart, J. N. Fox, I. Shaked, D. Heudobler, C. R. Raetz, E. W. Wang, S. L. Kelly, M. C. Sullards, R. C. Murphy, A. H. Merrill, Jr., H. A. Brown, E. A. Dennis, A. C. Li, K. Ley, S. Tsimikas, E. Fahy, S. Subramaniam, O. Quehenberger, D. W. Russell, and C. K. Glass.** 2012. Regulated accumulation of desmosterol integrates macrophage lipid metabolism and inflammatory responses. Cell **151:**138-52.

50. **Subramanian, A., P. Tamayo, V. K. Mootha, S. Mukherjee, B. L. Ebert, M. A. Gillette, A. Paulovich, S. L. Pomeroy, T. R. Golub, E. S. Lander, and J. P. Mesirov.** 2005. Gene set enrichment analysis: a knowledge-based approach for interpreting genome-wide expression profiles. Proc Natl Acad Sci U S A **102:**15545-50.

51. **Tavazoie, M. F., I. Pollack, R. Tanqueco, B. N. Ostendorf, B. S. Reis, F. C. Gonsalves, I. Kurth, C. Andreu-Agullo, M. L. Derbyshire, J. Posada, S. Takeda, K. N. Tafreshian, E. Rowinsky, M. Szarek, R. J. Waltzman, E. A. McMillan, C. Zhao, M. Mita, A. Mita, B. Chmielowski, M. A. Postow, A. Ribas, D. Mucida, and S. F. Tavazoie.** 2018. LXR/ApoE Activation Restricts Innate Immune Suppression in Cancer. Cell **172:**825-840.e18.

52. **Thorvaldsdottir, H., J. T. Robinson, and J. P. Mesirov.** 2013. Integrative Genomics Viewer (IGV): high-performance genomics data visualization and exploration. Brief Bioinform **14:**178-92.

53. **Tian, J., J. L. Goldstein, and M. S. Brown.** 2016. Insulin induction of SREBP-1c in rodent liver requires LXRalpha-C/EBPbeta complex. Proc Natl Acad Sci U S A **113:**8182-7.

54. **Valledor, A. F., L. C. Hsu, S. Ogawa, D. Sawka-Verhelle, M. Karin, and C. K. Glass.** 2004. Activation of liver X receptors and retinoid X receptors prevents bacterial-induced macrophage apoptosis. Proc Natl Acad Sci U S A **101:**17813-8.

55. **van de Laar, L., W. Saelens, S. De Prijck, L. Martens, C. L. Scott, G. Van Isterdael, E. Hoffmann, R. Beyaert, Y. Saeys, B. N. Lambrecht, and M. Guilliams.** 2016. Yolk Sac Macrophages, Fetal Liver, and Adult Monocytes Can Colonize an Empty Niche and Develop into Functional Tissue-Resident Macrophages. Immunity **44:**755-68.

56. **Venkateswaran, A., B. A. Laffitte, S. B. Joseph, P. A. Mak, D. C. Wilpitz, P. A. Edwards, and P. Tontonoz.** 2000. Control of cellular cholesterol efflux by the nuclear oxysterol receptor LXR alpha. Proc Natl Acad Sci U S A **97:**12097-102.

57. **Venteclef, N., T. Jakobsson, A. Ehrlund, A. Damdimopoulos, L. Mikkonen, E. Ellis, L. M. Nilsson, P. Parini, O. A. Janne, J. A. Gustafsson, K. R. Steffensen, and E. Treuter.** 2010. GPS2-dependent corepressor/SUMO pathways govern anti-inflammatory actions of LRH-1 and LXRbeta in the hepatic acute phase response. Genes Dev **24:**381-95.

58. **Wagner, B. L., A. F. Valledor, G. Shao, C. L. Daige, E. D. Bischoff, M. Petrowski, K. Jepsen, S. H. Baek, R. A. Heyman, M. G. Rosenfeld, I. G. Schulman, and C. K. Glass.** 2003. Promoter-specific roles for liver X receptor/corepressor complexes in the regulation of ABCA1 and SREBP1 gene expression. Mol Cell Biol **23:**5780-9.

59. **Walczak, R., S. B. Joseph, B. A. Laffitte, A. Castrillo, L. Pei, and P. Tontonoz.** 2004. Transcription of the vascular endothelial growth factor gene in macrophages is regulated by liver X receptors. J Biol Chem **279:**9905-11.

60. **Wang, B., and P. Tontonoz.** 2018. Liver X receptors in lipid signalling and membrane homeostasis. Nat Rev Endocrinol.

61. **Wang, J., Q. Sun, Y. Morita, H. Jiang, A. Gross, A. Lechel, K. Hildner, L. M. Guachalla, A. Gompf, D. Hartmann, A. Schambach, T. Wuestefeld, D. Dauch, H. Schrezenmeier, W. K. Hofmann, H. Nakauchi, Z. Ju, H. A. Kestler, L. Zender, and K. L. Rudolph.** 2012. A differentiation checkpoint limits hematopoietic stem cell self-renewal in response to DNA damage. Cell **148:**1001-14.

62. **Willy, P. J., K. Umesono, E. S. Ong, R. M. Evans, R. A. Heyman, and D. J. Mangelsdorf.** 1995. LXR, a nuclear receptor that defines a distinct retinoid response pathway. Genes Dev **9:**1033-45.
63. **Ye, T., S. Ravens, A. R. Krebs, and L. Tora.** 2014. Interpreting and visualizing ChIP-seq data with the seqMINER software. Methods Mol Biol **1150:**141-52.
64. **Yoshikawa, T., H. Shimano, M. Amemiya-Kudo, N. Yahagi, A. H. Hasty, T. Matsuzaka, H. Okazaki, Y. Tamura, Y. Iizuka, K. Ohashi, J. Osuga, K. Harada, T. Gotoda, S. Kimura, S. Ishibashi, and N. Yamada.** 2001. Identification of liver X receptor-retinoid X receptor as an activator of the sterol regulatory element-binding protein 1c gene promoter. Mol Cell Biol **21:**2991-3000.
65. **Zhang, Y., S. R. Breevoort, J. Angdisen, M. Fu, D. R. Schmidt, S. R. Holmstrom, S. A. Kliewer, D. J. Mangelsdorf, and I. G. Schulman.** 2012. Liver LXRalpha expression is crucial for whole body cholesterol homeostasis and reverse cholesterol transport in mice. J Clin Invest **122:**1688-99.
66. **Zuercher, W. J., R. G. Buckholz, N. Campobasso, J. L. Collins, C. M. Galardi, R. T. Gampe, S. M. Hyatt, S. L. Merrihew, J. T. Moore, J. A. Oplinger, P. R. Reid, P. K. Spearing, T. B. Stanley, E. L. Stewart, and T. M. Willson.** 2010. Discovery of tertiary sulfonamides as potent liver X receptor antagonists. Journal of Medicinal Chemistry **53:**3412-3416.

784 **FIGURES LEGENDS**

785

786 **Figure 1. Protein and RNA levels of LXRα and LXRβ in different *in vitro* macrophage models.**
787 Expression levels of LXRα, LXRβ, ABCA1 and ABCG1 from murine thioglycollate-elicited peritoneal
788 macrophages and bone marrow-derived macrophages differentiated with M-CSF and GM-CSF
789 cytokines were tested by western blot after cell treatment with LXR and RXR synthetic ligands **(A)** and
790 by qPCR, under GW3965 ligand treatment conditions **(B)**. Drug antagonism mediated by GW233 on
791 LXR target gene expression was investigated on LXR-WT and LXR-DKO peritoneal murine
792 macrophages by western blot. Cells were cultured with GW3965 (1μM) or GW233 (1μM), alone or in
793 combination for 24 hours **(C)**. The ability of GW233 to target both LXR nuclear receptors was tested on
794 LXR-WT and LXR single-knockout macrophage cells under similar culture conditions as in (C) **(D)**. One
795 representative experiment out of three is presented in each case, mean (SD) values of qPCR triplicates
796 are shown in (B).

797 **Figure 2. Reconstitution of LXRα and LXRβ expression in immortalized macrophages from LXR-**
798 **DKO bone marrow.**
799 **(A)** Outline of the experimental design for the generation of immortalized macrophage cell lines,
800 iBMDMs, expressing FLAG-tagged LXRα, LXRβ or no LXR receptors. **(B, left panel)** Whole protein
801 extracts from iBMDM-LXR macrophages cultured under different serum-depletion conditions (see
802 "Materials and Methods") were analyzed by western blot for the expression of virally transduced LXRα
803 or LXRβ. Induction levels of the LXR target genes ABCA1 and ABCG1 were also examined. GAPDH
804 was used as loading control. **(B, right panel)** LXRα and LXRβ protein expression was tested in whole
805 protein extracts from iBMDM macrophages, RAW cells virally transduced with LXRα **(26)** and WT
806 peritoneal macrophages, treated with GW3965 (1μM). β-actin was used as loading control. Dashed line
807 box in LXRα/β panel indicates specific 3FLAG-LXRα protein band, which shows a slightly similar weight
808 as endogenous LXRβ protein. **(C)** Expression of dual and LXRα-specific (*Cd5l*) target genes upon
809 GW3965 or GW233 (1μM) treatment was examined by real-time qPCR. Results are represented as
810 mean (±SD) values of three independent experiments. Asterisks indicate statistical significance
811 between treatments *p<0.05 and **p<0.01.

812 **Figure 3. LXRα/β ligand-induced binding and histone H3 acetylation in the cis-acting regulatory**
813 **regions of known LXR target genes.**
814 **(A)** LXR occupancy was detected in the regulatory sites of known target genes in iBMDM macrophages
815 using anti-FLAG antibody. Data are expressed as mean (±SD) values of three independent
816 experiments. Asterisks indicate statistical significance relative to an irrelevant distal region, *p<0.05 and
817 **p<0.01. **(B)** LXRα/β binding capacity to LXR regulatory sites was tested in cells cultured with GW3965
818 and GW233 (24h, 1μM). Data are expressed as mean (±SD) values of two independent experiments.
819 **(C)** Acetylation/deacetylation dynamics of histone H3 (H3K27ac) upon iBMDM treatment with GW3965
820 and GW233 was examined by ChIP-qPCR. Statistical significance was calculated between treatments
821 in each iBMDM-LXR cell line with unpaired Student´s t-test *p<0.05 and **p<0.01.

Figure 4. Genome-wide occupancy of LXRα and LXRβ nuclear receptors in iBMDM cells.
(A) Genomic binding locations of LXRα and LXRβ nuclear receptors in iBMDM macrophages are represented in a scatter plot by receptor normalized ChIP-seq tag counts (Log_2). **(B)** Number of unique and shared genomic LXR-bound sites, depicted as Venn diagram. **(C)** Distribution of LXRα, LXRβ and shared LXRα/β binding sites in reference to gene features are shown. TSS, transcription start site; TTS, transcription termination site. **(D)** Density heatmap of LXRα, LXRβ and RXRα ChIP-seq peak intensities in a 2Kb window, detected in iBMDM and primary macrophages (accession number GSE63698), respectively. Genomic regions are clustered according to shared LXRα/β, LXRα and LXRβ-specific occupancies. **(E)** LXR and RXR binding (ChIP sequencing tags per bp) in dual, LXRα and LXRβ peak clusters. **(F)** Top-five *de novo* and known sequence motif enrichment associated to LXR/RXRα-bound sites in iBMDM macrophages (see supplementary table 2 for complete list).

Figure 5. Genome-wide co-localization of LXRα/β binding peaks and their corresponding H3K27ac marks in iBMDM macrophages.
(A) Changes in acetylation marks (H3K27ac) upon agonist and antagonist drug treatment of iBMDM macrophages were examined by ChIP-seq. Acetylated areas are represented as a density heatmap, within a 2Kb window of centred LXRα/β, LXRα and LXRβ peaks as described in Fig 4D. LXR peak-associated acetylated genomic regions are subdivided into six clusters (C1 to C6) and arranged depending on pharmacological responsiveness. Clusters C1, C3 and C5: pharmacologically responsive acetylation marks; clusters C2, C4 and C6: weakly or non-responsive acetylated regions. Top *De novo* sequence motifs identified in clusters C1-C6 and their associated p-values are indicated. **(B)** Box plot representation of genomic mean changes in H3K27ac mark intensity, measured as normalized tag counts (Log_2) in LXR peak sub clusters (C1-C6), after GW3965 and GW233 stimulation and p-value changes.

Figure 6. Expression profiling uncovers LXR dual and isoform-specific targets and reveals putative LXR transcriptional modes of action in response to agonist/antagonist.
Microarray analysis in iBMDM macrophages was performed using GW3965 and GW233 culture conditions as described in “Materials and Methods”. Heatmap representation (panels on the left) shows fold changes in response to GW3965 relative to GW233 in each iBMDM cell line. An alternative heatmap representation (panels on the right) shows gene expression of each drug treatment relative to LXR-DKO iBMDMs. Relativized data highlight three possible mechanisms of LXRα/β **(A)**, LXRα **(B)** and LXRβ **(C)** -mediated gene activation (modes I, II, III). The number of transcripts induced by each mechanism is indicated on the left side. Lower panels show UCSC Genome Browser snapshots of representative genes as examples of each mechanism.

Figure 7. Gene Ontology analysis and IPA pathway annotation to microarray gene clusters.
Biological pathway analysis was performed on genes that belong to: pharmacologically responsive (up in GW3965/GW233 ratio: modes I and II) and non-responsive (up when referred to iBMDM-DKO: mode III) clusters. **(A)** Most relevant IPA biological pathways associated to modes I and II (pharmacologically responsive) are depicted as a heatmap. Below, additional relevant GO terms and functions identified by

IPA are shown. **(B)** Most relevant IPA biological pathways associated to mode III (pharmacologically non-responsive) are depicted as a heatmap. Pathways were arranged by receptor dependence. Right table shows additional relevant GO terms and IPA functions. Right-tailed Fisher's Exact Test p-values for each case are shown. The highest, lowest and borderline statistical significant p-values are shown for each category.

Figure 8. Upstream signaling pathways connecting gene expression cascades triggered by LXR activity in a pharmacological-dependent manner (Modes I and II).
(A) Molecular regulators of gene expression networks associated to transcriptional modes I and II, identified with IPA. Heatmap color intensities correlate with significance of right-tailed Fisher's Exact Test. **(B)** Diagrams showing molecular interaction networks between signaling regulators and pharmacologically active LXRα and LXRβ, leading to gene expression cascades. Predicted relationships among molecules yielded by IPA are indicated. The highest and lowest statistical significant p-values are shown for each category.

Figure 9. Upstream signaling pathways connecting gene expression cascades triggered by LXR activity in a pharmacologically-independent manner (Mode III).
(A) Molecular regulators of gene expression networks associated to transcriptional mode III, identified with IPA. Heatmap colour intensities correlate with significance of right-tailed Fisher's Exact Test. **(B)** Diagrams showing molecular interaction networks between signaling regulators and LXR receptors. Predicted relationships among molecules yielded by IPA are indicated. The highest and lowest statistical significant p-values are shown for each category.

Figure 10. Proposed mechanisms for LXR nuclear receptors transcriptional activation. Through integration of gene expression and genome binding data, three possible transcriptional LXR-mediated mechanisms or modes (namely I, II, III) are proposed.

Figure 1

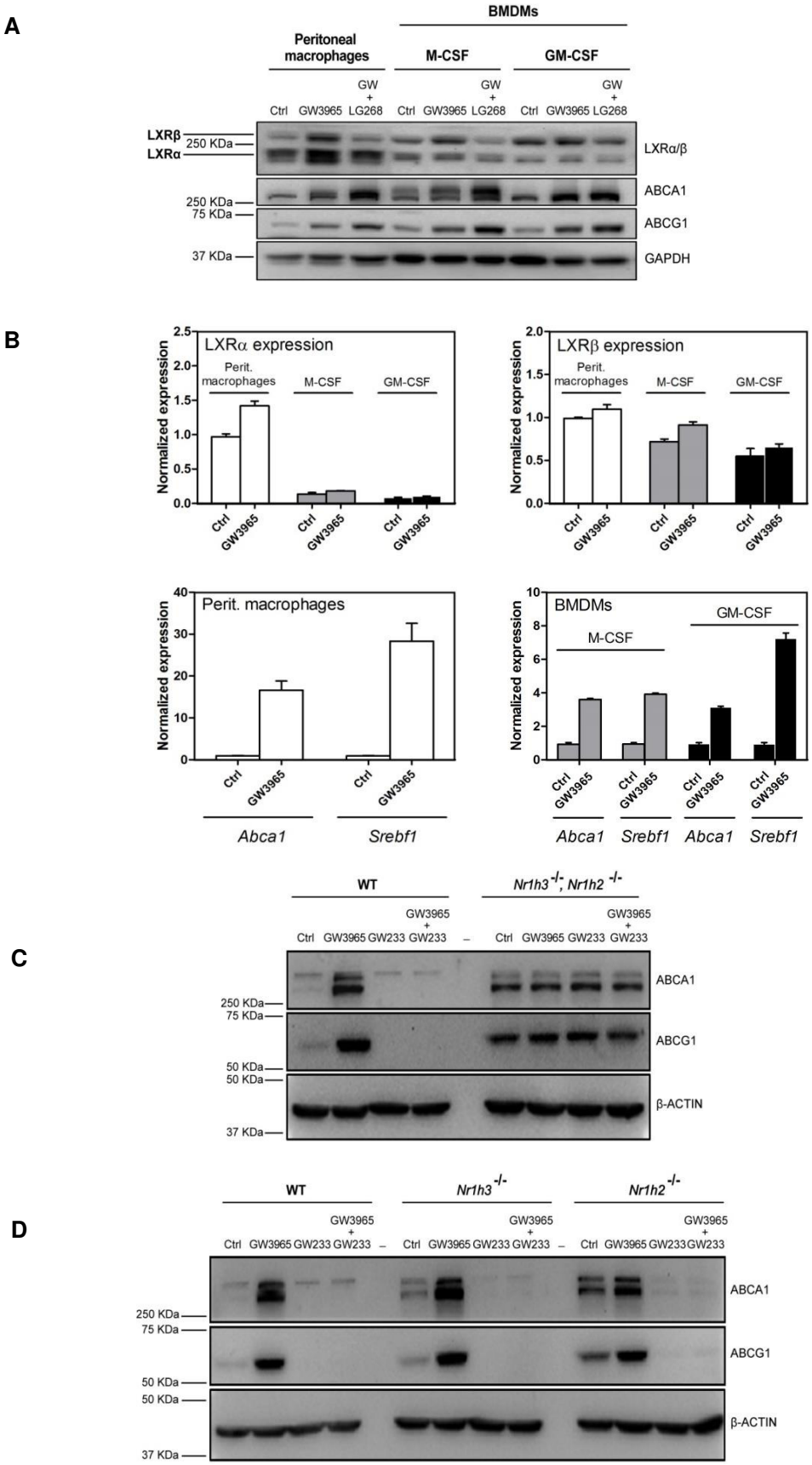

Figure 2

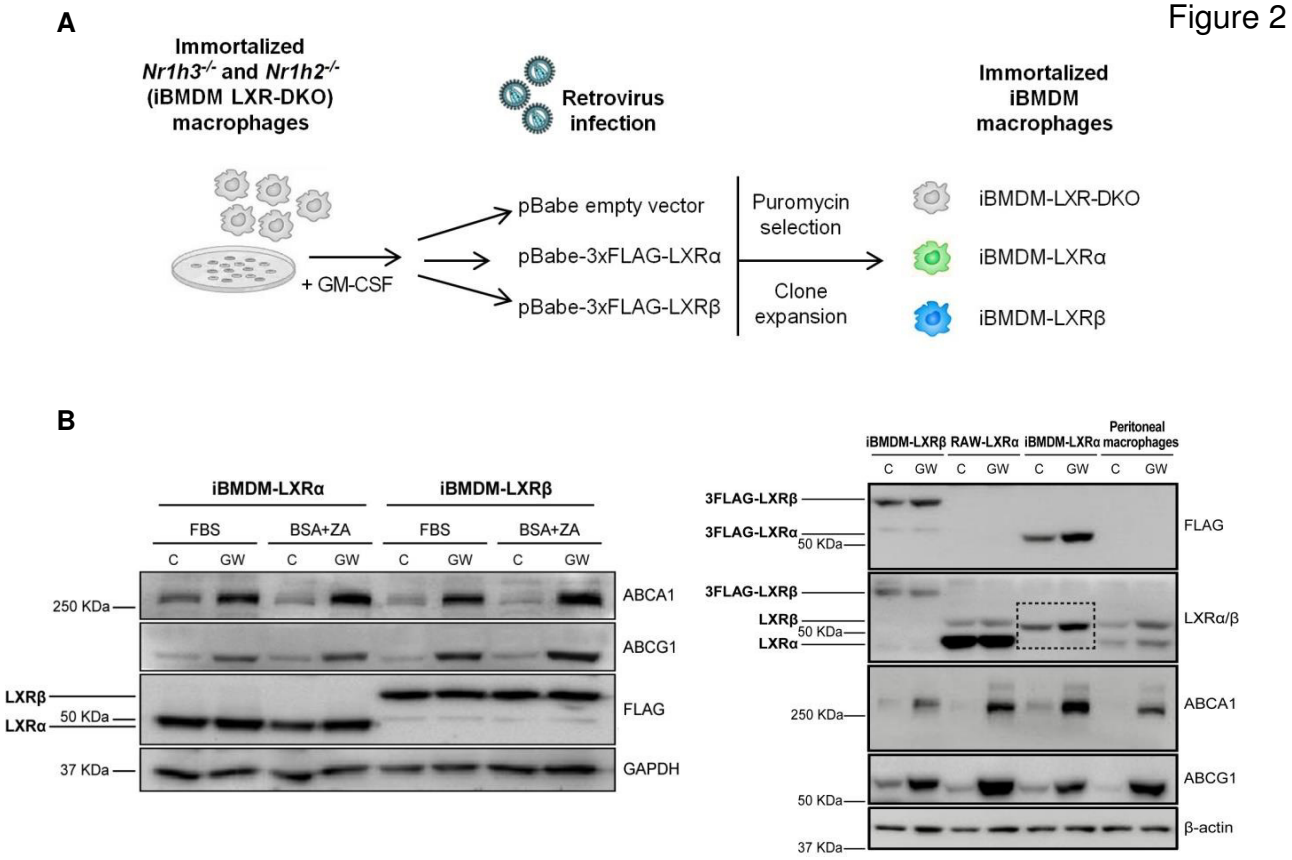

Figure 3

A

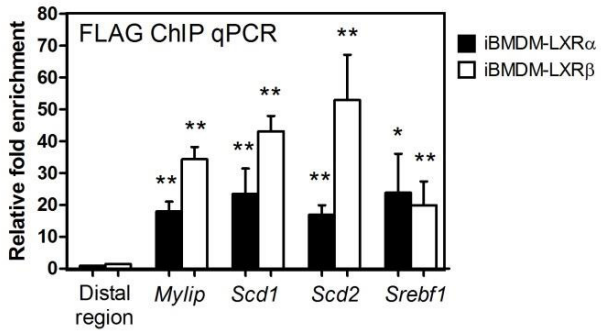

B

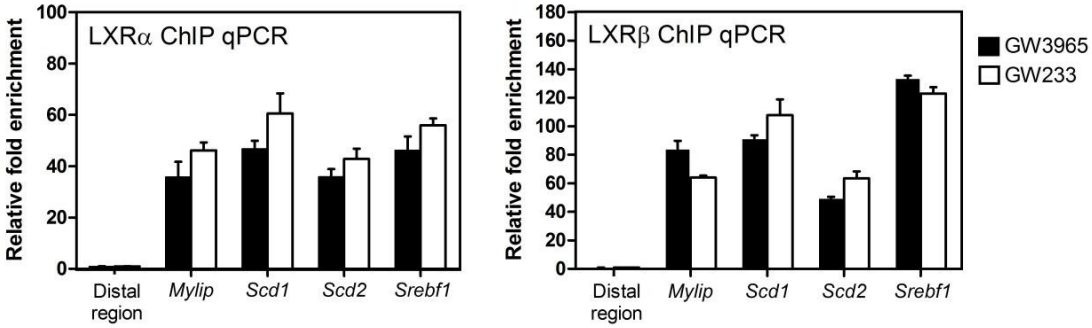

C

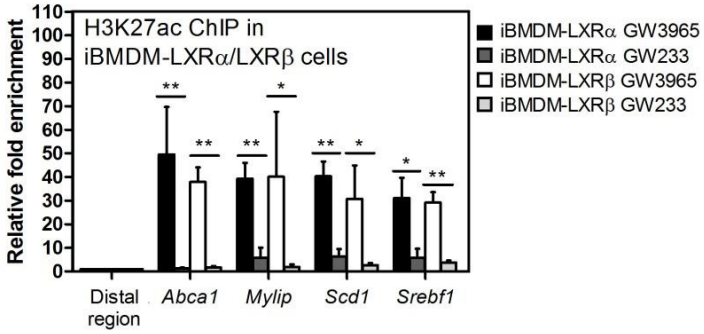

Figure 4

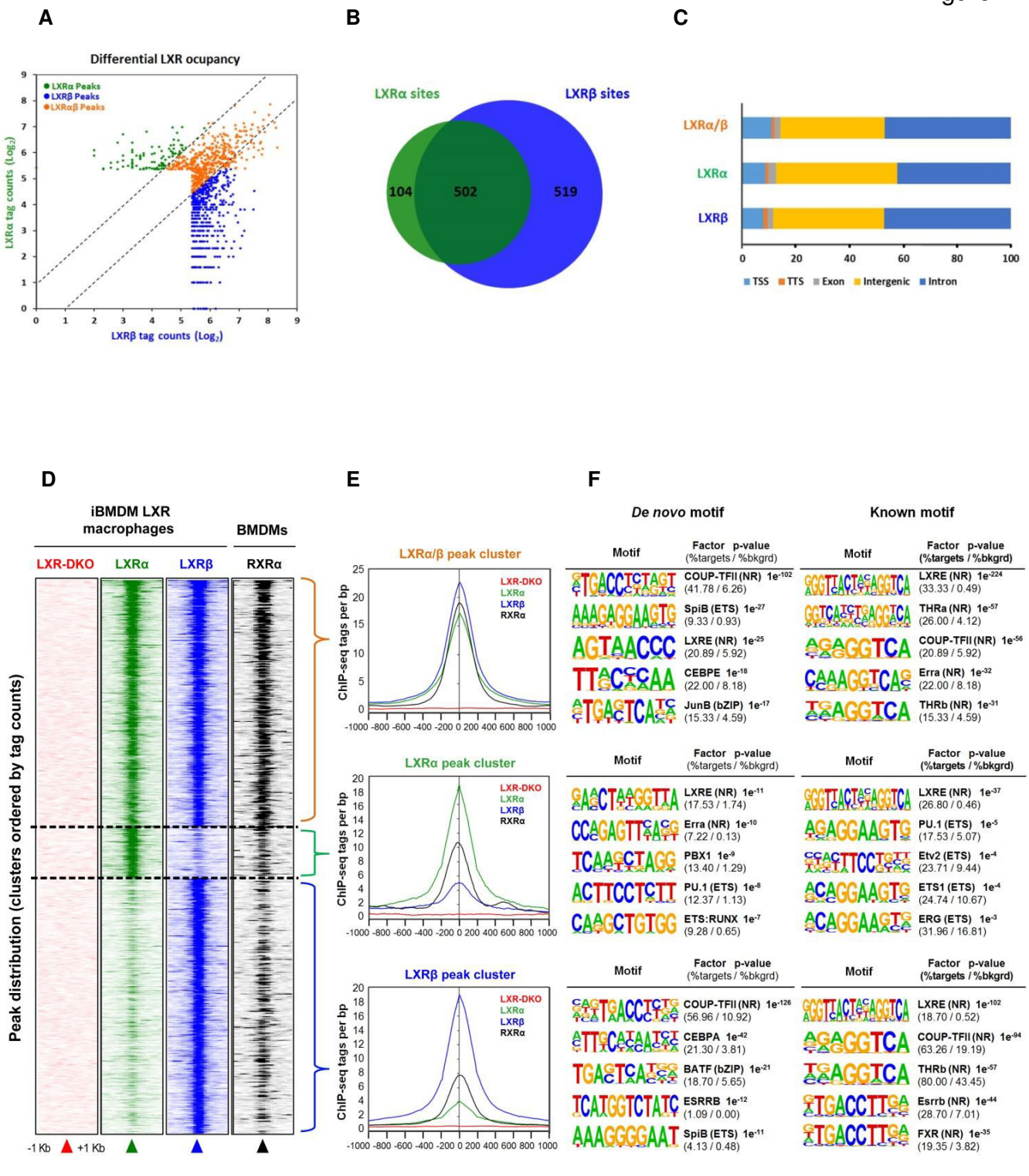

Figure 5

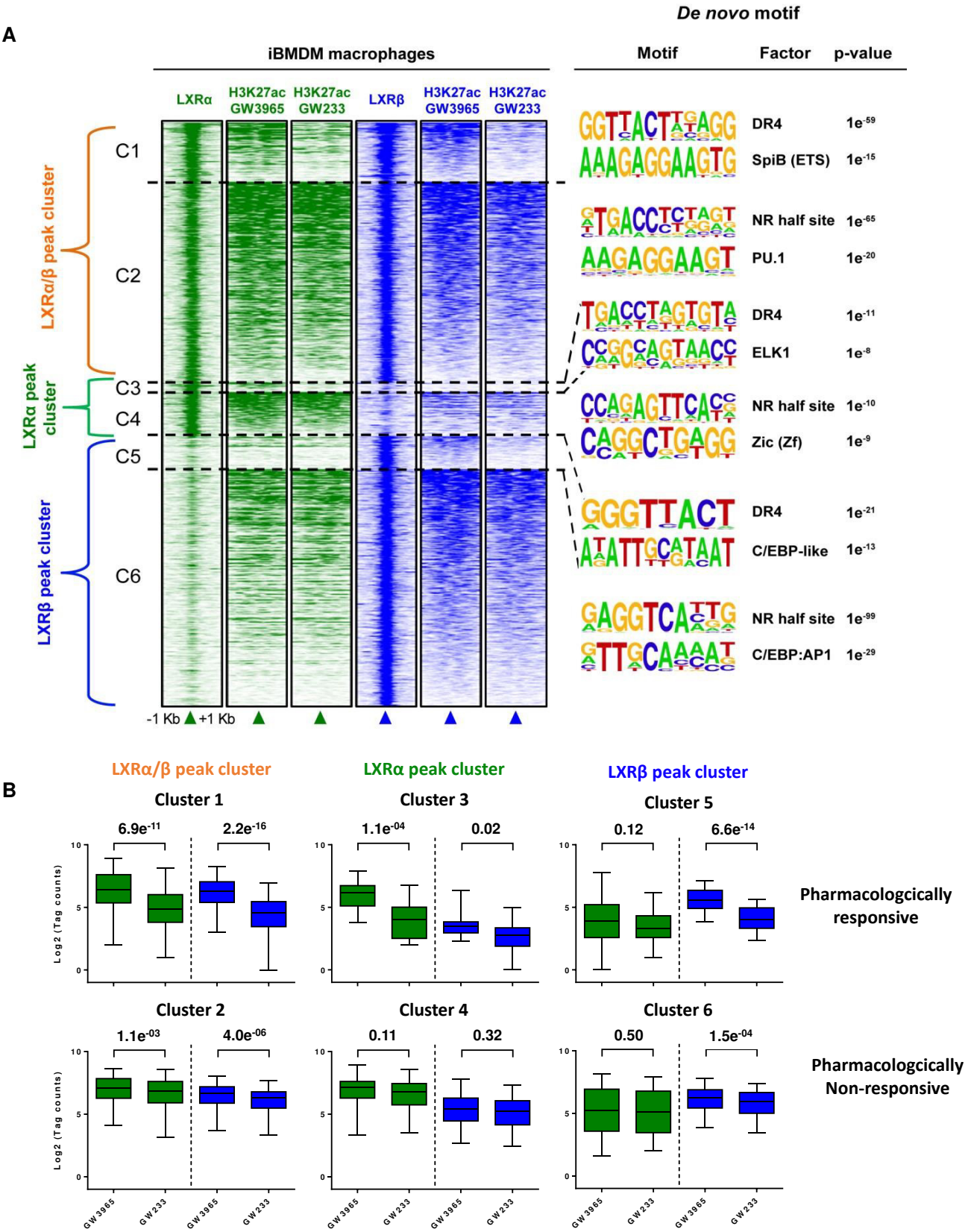

Figure 6

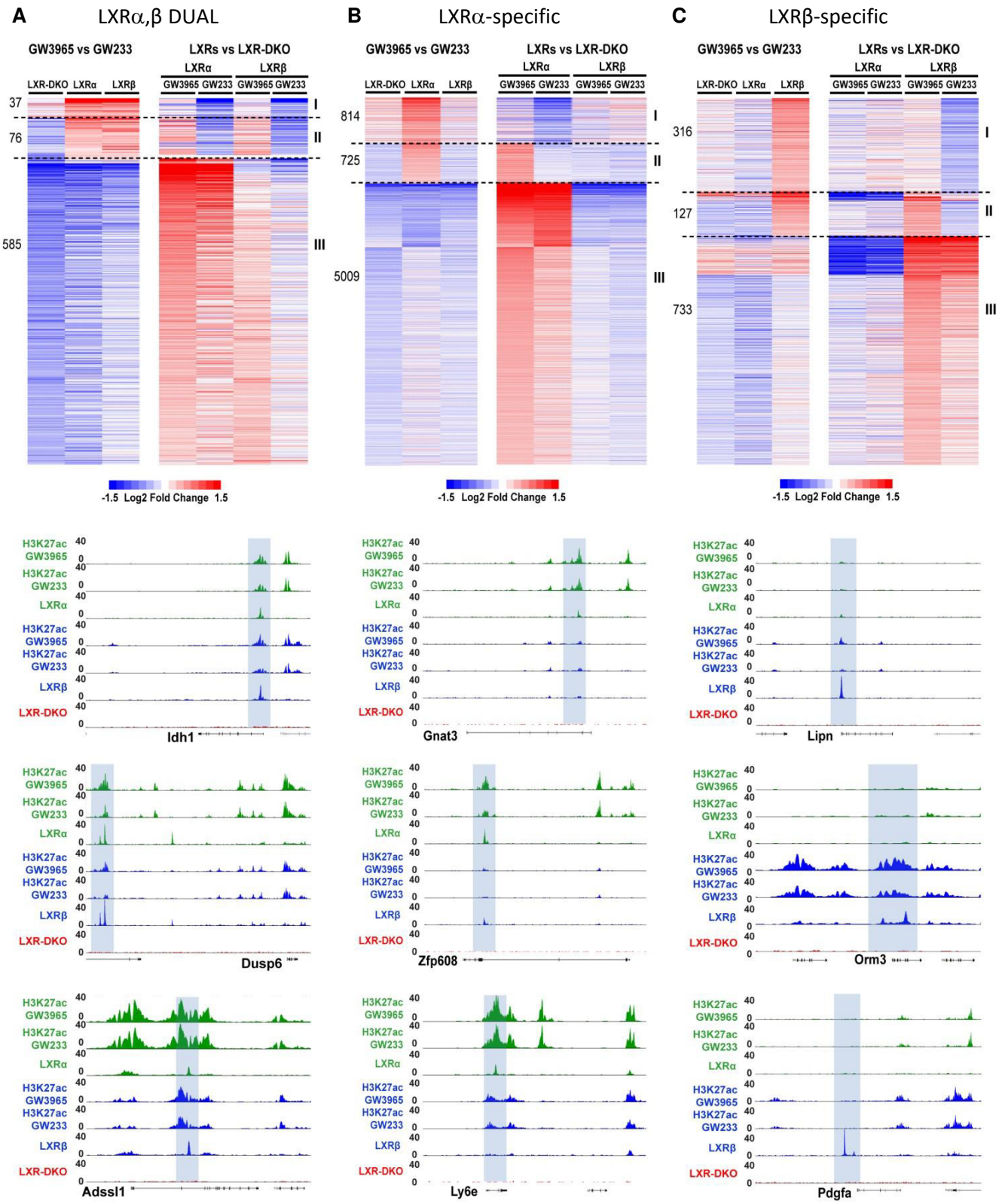

Figure 7

A Biological pathways identified in pharmacologically-responsive clusters (modes I and II)

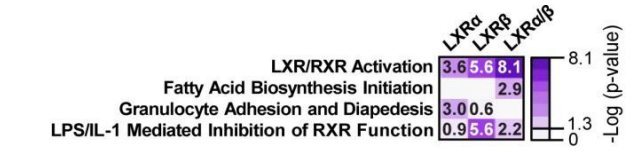

	GO Terms	p-value	IPA pathways/functions	p-value
LXRα	Regulation of lipid metabolic process	2.54E-05	Migration of myeloid cells	1.80E-06
	Regulation of steroid metabolic process	1.43E-04	Fatty acid metabolism	7.64E-05
	Positive regulation of leukocyte migration	3.72E-04	Synthesis of steroid	2.48E-03
LXRβ	Vesicle-mediated transport	1.80E-05	Activation of leukocytes	8.32E-07
	VLDL particle clearance	2.75E-05	Clathrin-mediated endocytosis signaling	5.68E-03
	Acute-phase response	4.89E-05	Acute Phase Response signaling	3.78E-02
LXRα/β	Positive regulation of steroid metabolic process	8.53E-07	Synthesis of sterol	4.05E-06
	Regulation of protein stability	2.31E-04	Unfolded protein response	3.73E-02

B Biological pathways identified in pharmacologically non-responsive cluster (mode III)

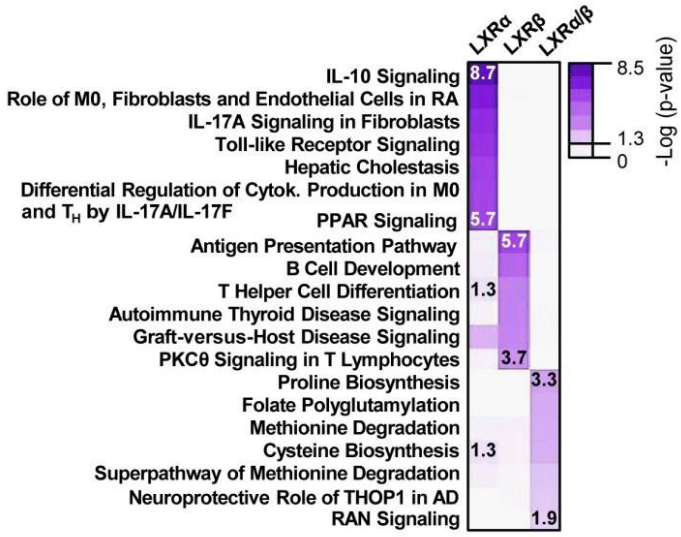

	GO Terms	p-value
LXRα	Apoptosis	4.07E-26
	Inflammatory response	5.28E-22
	Cell migration	1.91E-19
LXRβ	Selection of thymocytes	1.83E-03
	Morphology of lymph node	4.04E-03
	Transport of iron ion	6.43E-03
LXRα/β	rRNA processing	4.16E-04
	DNA replication involved in S phase	5.58E-03
	IPA pathways/functions	**p-value**
LXRα	Cell movement	3.13E-33
	Inflammatory response	1.42E-25
	Apoptosis	4.36E-24
LXRβ	Cellular response to iron ion	3.97E-03
	Immune system development	1.23E-02
	Lymphocyte differentiation	1.29E-02
LXRα/β	Initiation of replication of DNA	1.03E-03
	Transcription of rRNA	8.92E-03

Molecular and Cellular Biology

A Bioinformatic prediction of upstream signaling pathways involved in mode I, II clusters

Figure 8

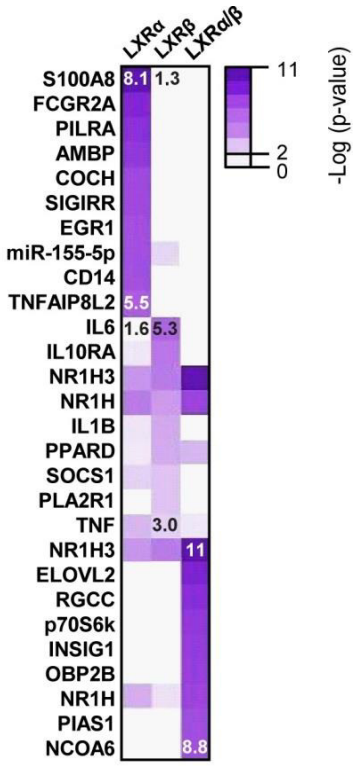

B Molecular connections between upstream regulators and LXRα-dependent gene expression (modes I and II)

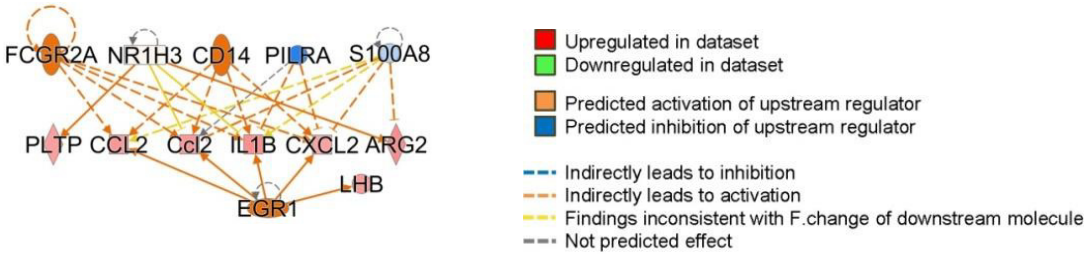

Molecular connections between upstream regulators and LXRβ-dependent gene expression (modes I and II)

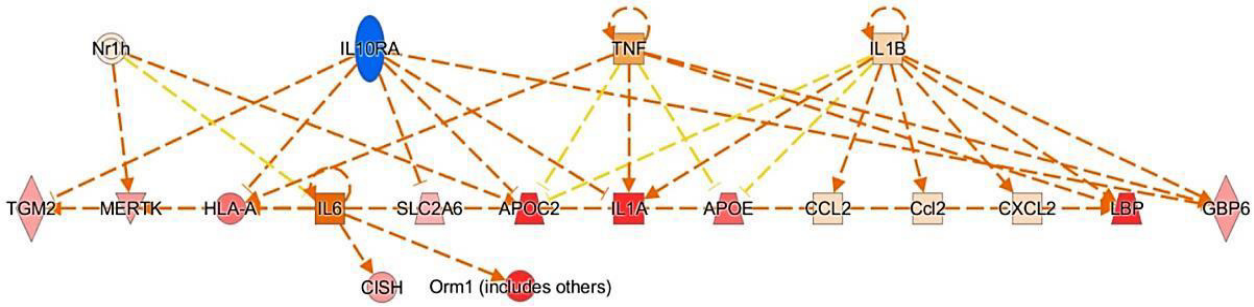

A Bioinformatic prediction of upstream signaling pathways involved in mode III cluster

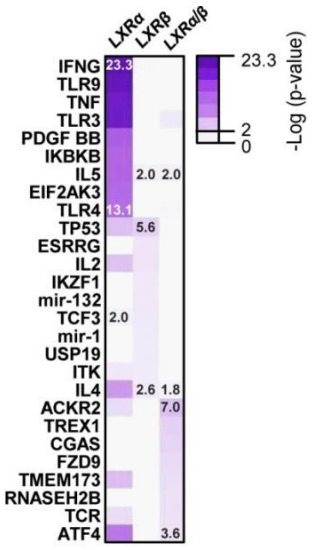

Figure 9

B Molecular connections between upstream regulators and mode III clusters

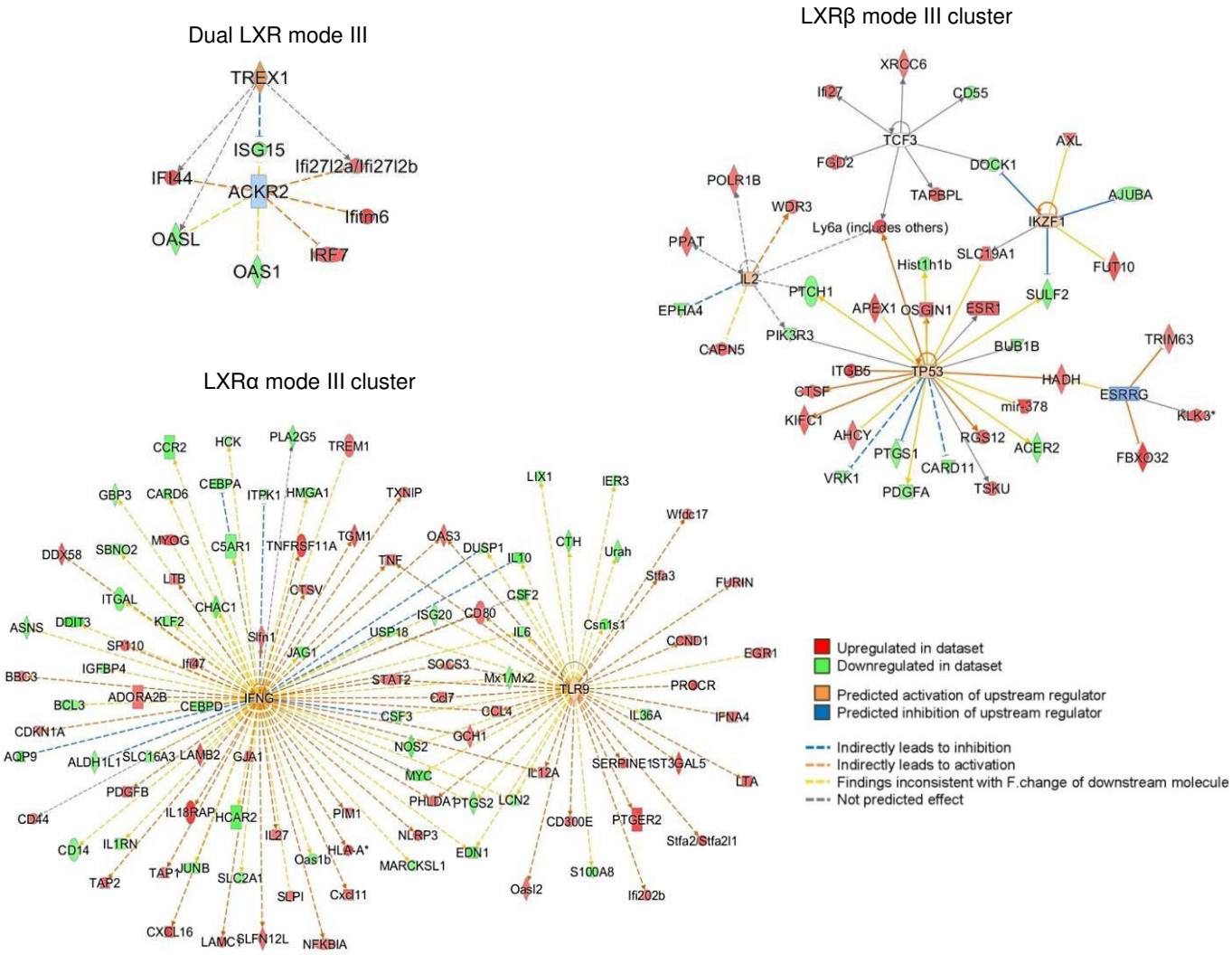

Figure 10